The NONLINEAR M3D-C^1 Code with application to disruptive beta limits in NSTX

Stephen C. Jardin[1]
N.M. Ferraro[2], J. Chen[1], J. Breslau[1]

[1]*Princeton Plasma Physics Laboratory*
[2] *General Atomics*

June 24, 2013

This work was performed in close collaboration with M. Shephard, F. Zhang, and others at the SCOREC center at Rensselaer Polytechnic Institute in Troy, NY.

Acknowledgements also to: G. Fu, S. Hudson, W. Park, H. Strauss, L. Sugiyama.

B. Lyons and J. Ramos are incorporating neoclassical effects into M3D-C^1

PPPL PRINCETON PLASMA PHYSICS LABORATORY

motivation

- What causes a plasma to disrupt?
- Linear stability to all global modes for all time will ensure disruption-free operation.
- However, the converse is not true.
  - Linear instability does not necessarily imply a disruption.
- Can we use a non-linear MHD code to identify nonlinear events that lead to a disruption (or not)?

Outline

- Summary of features of NONLINEAR M3D-C^1 code

- Nonlinear simulations of exceeding the linear stability limit (β-limit) in NSTX shot 124379 at late times

- Review of application to sawtooth and stationary states with $q_0 \cong 1$ (time permiting)

- Summary and future directions

M3D-C^1 code

- High accuracy
  - High order finite elements in 3D with C^1 continuity
  - Optimal decomposition of vector fields into scalars
  - Full 2F MHD equations without common approximations
  - Accuracy of linear flux-coordinate (FC) codes without using FC
- Long-time simulations (large time steps)
  - Requires fully implicit algorithm
  - Unique preconditioning techniques
- Geometrical flexibility
  - Unstructured mesh allows variable mesh size (mesh packing)
  - Does not use flux coordinates → Plasma region with seperatrix
  - Arbitrary shaped vacuum vessel and conductors

For magnetic confinement, there are 4 classes of major simulation codes, each addressing different phenomena

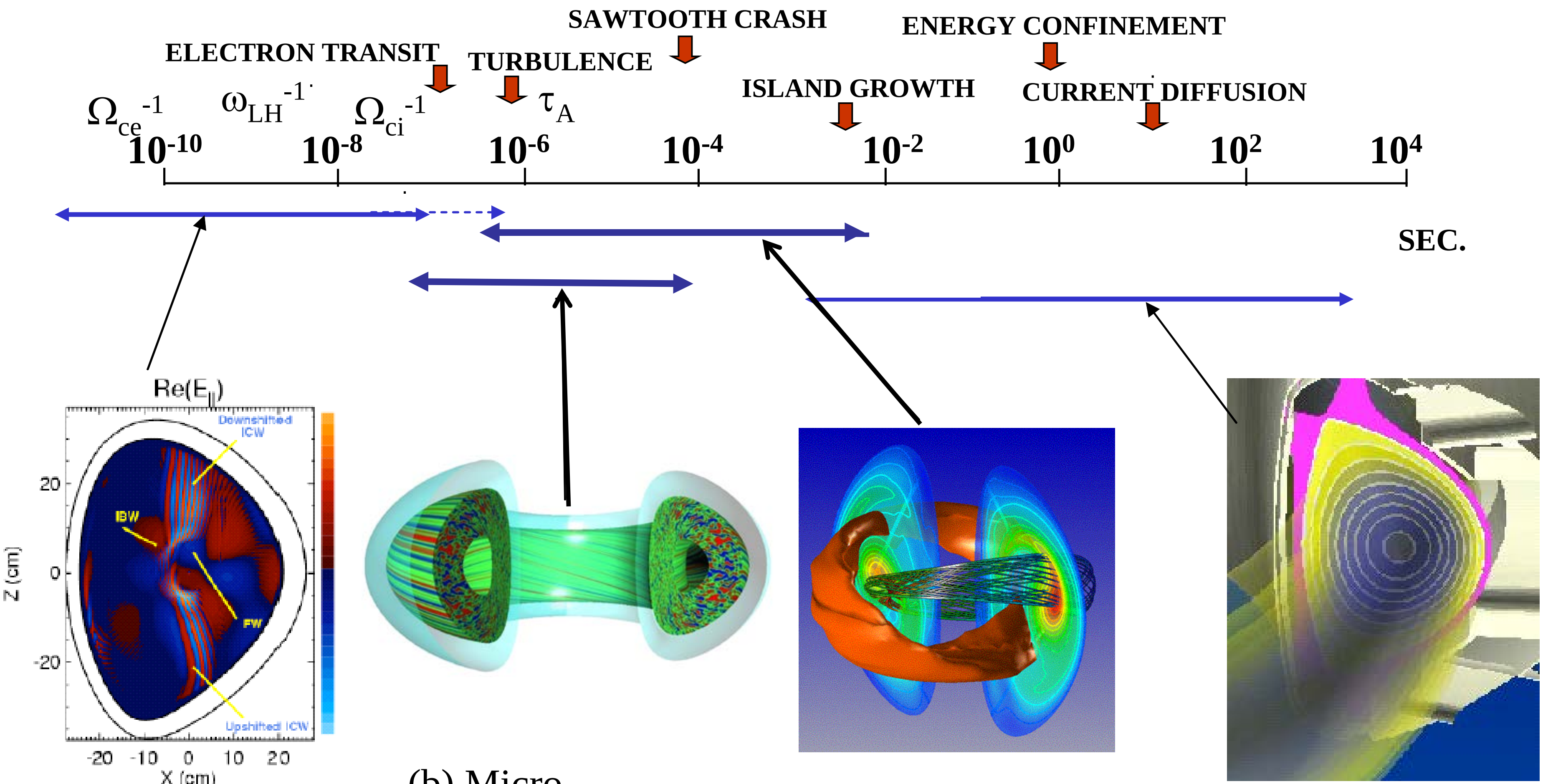

(a) RF codes

(b) Micro-turbulence codes

(c) Extended-MHD codes

(d) Transport Codes

For magnetic confinement, there are 4 classes of major simulation codes, each addressing different phenomena

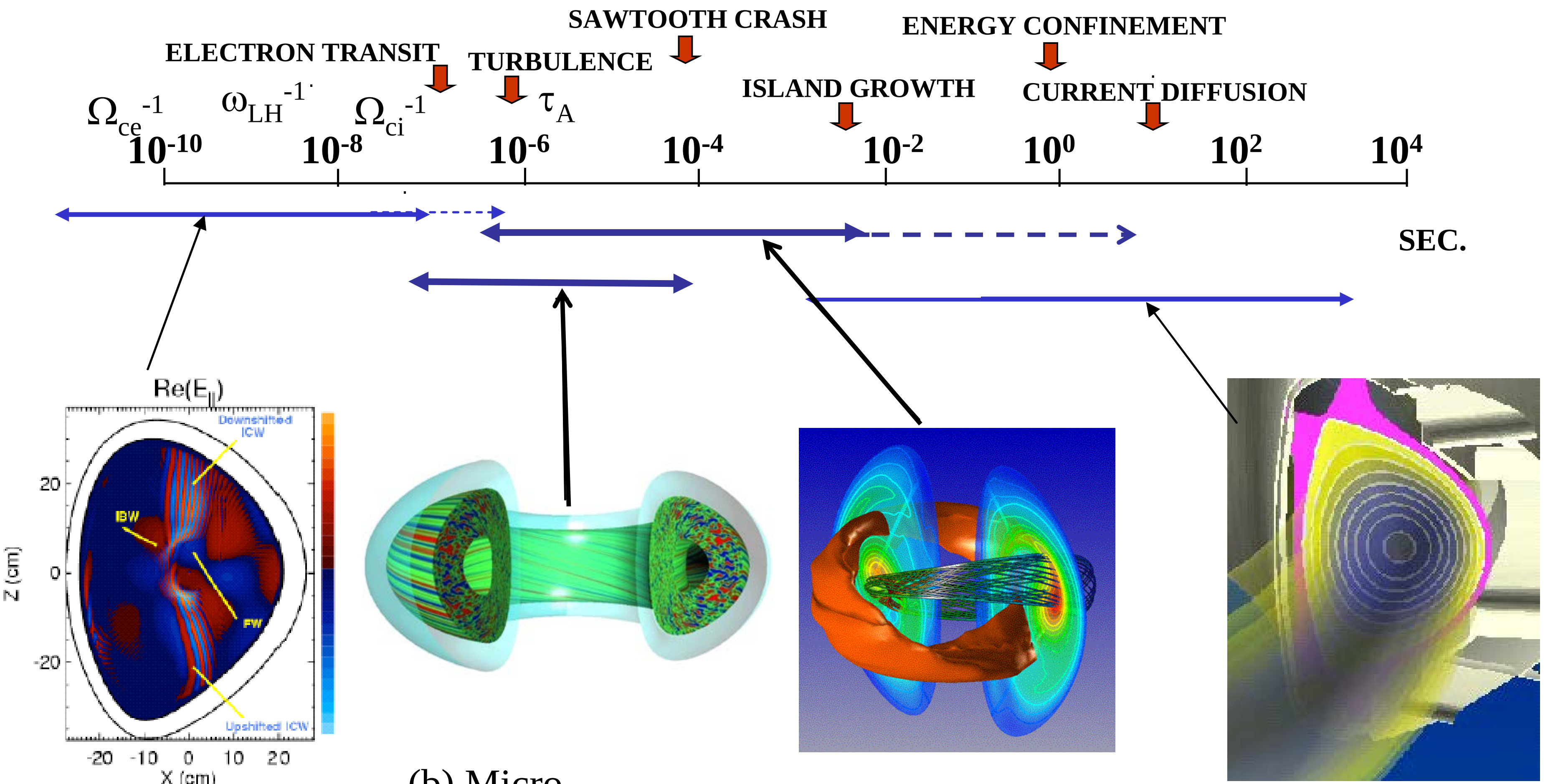

(a) RF codes

(b) Micro-turbulence codes

(c) Extended-MHD codes

(d) Transport Codes

A goal of the M3D-C^1 project is to extend the range of timescales for X-MHD codes so that transport and stability phenomena can be studied together.

2-Fluid 3D MHD Equations:

$$\frac{\partial n}{\partial t} + \nabla \bullet (n\mathbf{V}) = 0$$ continuity

$$\frac{\partial \mathbf{B}}{\partial t} = -\nabla \times \mathbf{E} \qquad \nabla \bullet \mathbf{B} = 0 \qquad \mu_0 \mathbf{J} = \nabla \times \mathbf{B}$$ Maxwell

$$nM_i\left(\frac{\partial \mathbf{V}}{\partial t} + \mathbf{V} \bullet \nabla \mathbf{V}\right) + \nabla p = \mathbf{J} \times \mathbf{B} - \nabla \bullet \mathbf{\Pi}_{GV} - \nabla \bullet \mathbf{\Pi}_{\mu}$$ momentum

$$\mathbf{E} + \mathbf{V} \times \mathbf{B} = \eta \mathbf{J} + \frac{1}{ne}\left(\mathbf{J} \times \mathbf{B} - \nabla p_e - \nabla \bullet \mathbf{\Pi}_e\right)$$ Ohm's law

$$\frac{3}{2}\frac{\partial p_e}{\partial t} + \nabla \bullet \left(\frac{3}{2} p_e \mathbf{V}\right) = -p_e \nabla \bullet \mathbf{V} + \eta J^2 - \nabla \bullet \mathbf{q}_e + Q_\Delta$$ electron energy

$$\frac{3}{2}\frac{\partial p_i}{\partial t} + \nabla \bullet \left(\frac{3}{2} p_i \mathbf{V}\right) = -p_i \nabla \bullet \mathbf{V} - \mathbf{\Pi}_\mu \bullet \nabla \mathbf{V} - \nabla \bullet \mathbf{q}_i - Q_\Delta$$ ion energy

Ideal MHD
Resistive MHD
2-fluid MHD

The objective of the **M3D-C^1** project is to solve these equations as accurately as possible in 3D toroidal geometry with realistic B.C. and for times long compared to τ_A Solution algorithm is optimized for a low-β torus with a strong toroidal field.

Contain ideal MHD, reconnection, and transport timescales

$$\tau_I \ll \tau_R \ll \tau_T$$

Form of the vector fields motivated by reduced MHD

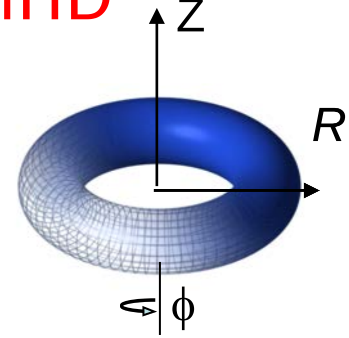

Velocity Field:

$$\mathbf{V} = R^2 \nabla U \times \nabla \phi + R^2 \omega \nabla \phi + \frac{1}{R^2} \nabla_\perp \chi$$

All components orthogonal !

$$\int |\mathbf{V}|^2 \, d\tau = \int \left[R^2 |\nabla_\perp U|^2 + R^2 \omega^2 + \frac{1}{R^4} |\nabla_\perp \chi|^2 \right] d\tau$$

This form separates the different MHD characteristics for greatly improved accuracy.

Magnetic vector potential:

$$\mathbf{A} = R^2 \nabla \phi \times \nabla f + \psi \nabla \phi - F_0 \ln R \hat{Z}$$

$$\mathbf{B} = \nabla \psi \times \nabla \phi - \nabla_\perp \frac{\partial f}{\partial \phi} + F \nabla \phi$$

$$= \nabla \psi \times \nabla \phi - \nabla \frac{\partial f}{\partial \phi} + F^* \nabla \phi$$

$$\mathbf{J} = \nabla F^* \times \nabla \phi + \frac{1}{R^2} \nabla_\perp \frac{\partial \psi}{\partial \phi} - \Delta^* \psi \nabla \phi$$

$$F \equiv F_0 + R^2 \nabla_\perp^2 f$$

$$F^* \equiv F_0 + R^2 \nabla^2 f$$

Only 2 scalar variables for the magnetic field and current

$\nabla \bullet \mathbf{B} = 0$ is built in

M3D-C^1 code can be run in several very different modes

Linearity and dimensionality:

- 2D nonlinear (Nate Ferraro's thesis)
  - need sources and controllers for current, density, energy
- 3D linear (single toroidal harmonic $e^{in\varphi}$, complex arithmetic)
- 3D nonlinear
  - with equilibrium subtracted out (assumes initial equilibrium is stationary in all equations on all timescales)
  - Or, without subtracting equilibrium (using controllers)

Full MHD or reduced MHD

$$\mathbf{V} = R^2 \nabla U \times \nabla \phi + R^2 \omega \nabla \phi + \frac{1}{R^2} \nabla_\perp \chi$$

$$\mathbf{A} = R^2 \nabla \phi \times \nabla f + \psi \nabla \phi - F_0 \ln R \hat{Z}$$

- NUMVAR=1 U, ψ
- NUMVAR=2 U, ω, ψ, f
- NUMVAR=3 full MHD $U, \omega, \chi, \psi, f, p_e, p_i, n$

Ideal MHD, Resistive MHD, or 2F MHD

Separate p_e and p_i and density (n) advance are optional

Meshing and elements:

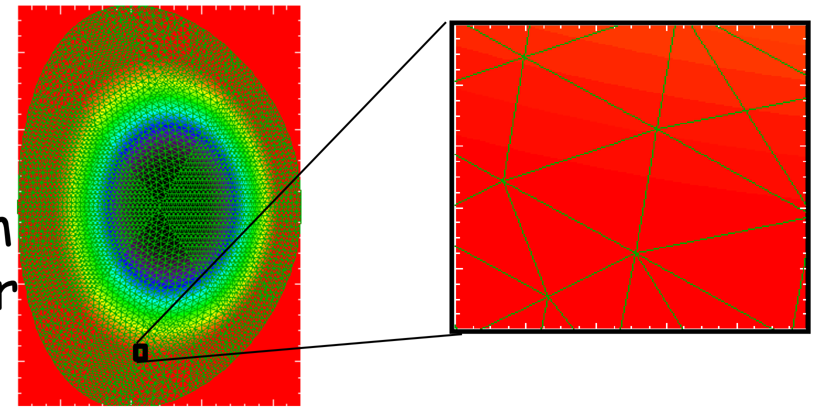

2D and 3D use unstructured high order triangular elements in the poloidal plane

These can be adapted using the equilibrium flux surfaces to give higher resolution near rational surfaces and edge

3D *linear* assumes toroidal dependence exp(inφ) for single n-mode

3D *non-linear* uses high order triangular wedge finite elements. For every scalar quantity, each element has polynomial in (R,φ,Z) with 72 terms constructed so that variable and first-derivatives are continuous across elements.

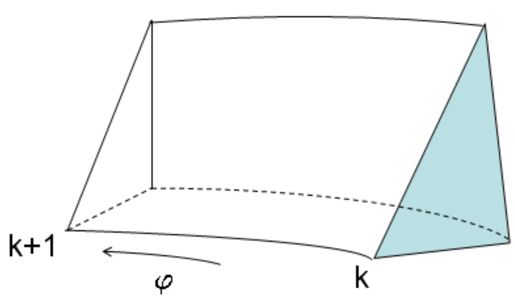

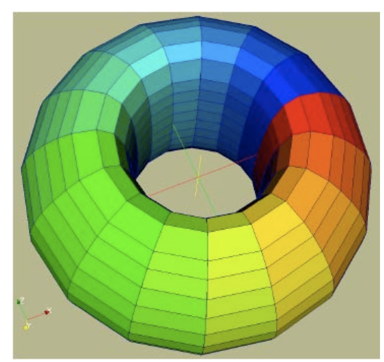

Initial Equilibrium:

Initial equilibrium is normally imported from geqdsk file and re-solved using high-order M3D-C^1 elements.

X-point is located, and seperatrix separates plasma from low temperature “vacuum”.

Grid can then be packed near edge or rational surfaces, and equilibrium is re-solved with the new grid.

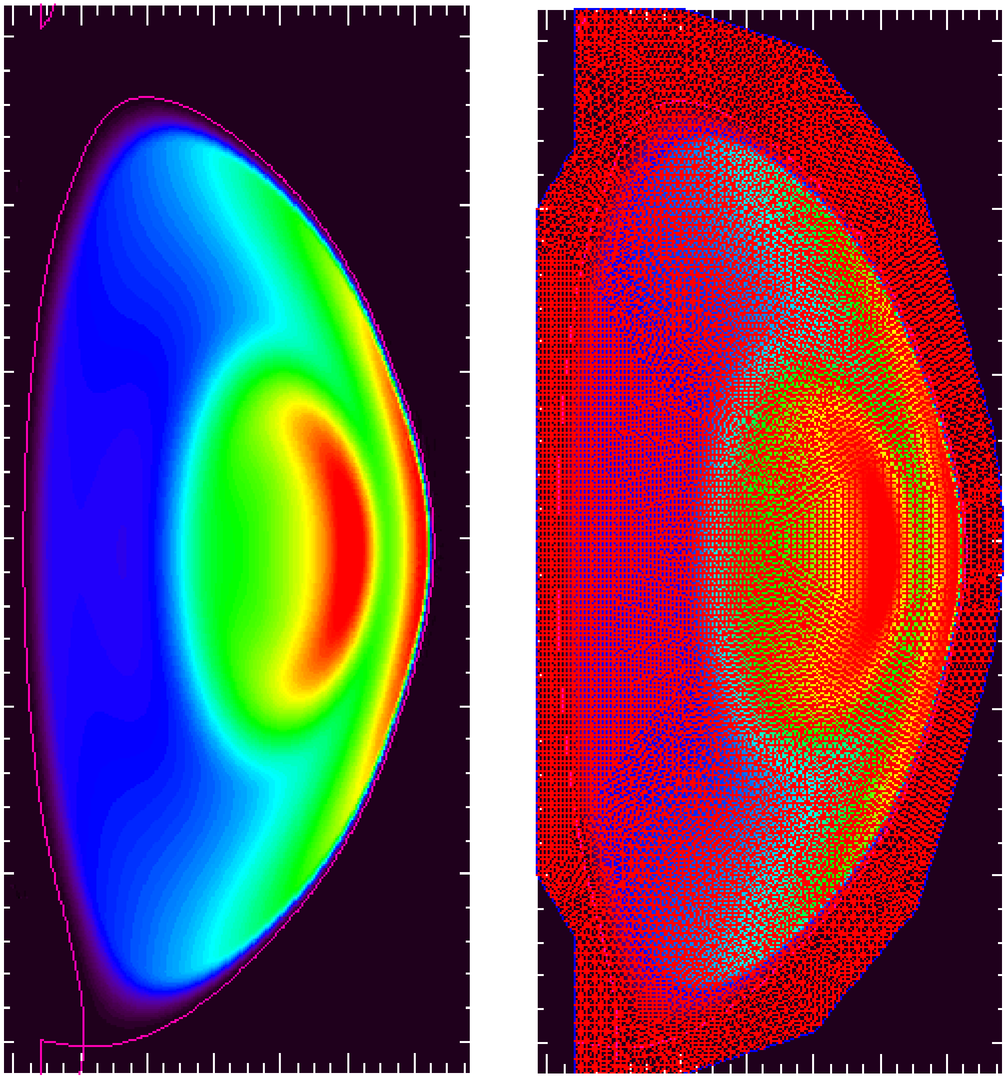

Jφ   Jφ (showing grid)

Implicit solution requires evaluating the spatial derivatives at the new time level.

The advantage of an implicit solution is that the time step can be very large and still be numerically stable (no Courant condition)

If we discretize in space (finite difference, finite element, or spectral) and linearize the equations about the present time level, the implicit equations take the form:

$$\begin{bmatrix} \mathbf{A}_{11} & \mathbf{A}_{12} & \mathbf{A}_{13} \\ \mathbf{A}_{21} & \mathbf{A}_{22} & \mathbf{A}_{23} \\ \mathbf{A}_{31} & \mathbf{A}_{32} & \mathbf{A}_{33} \end{bmatrix} \bullet \begin{bmatrix} \mathbf{V} \\ \mathbf{B} \\ p \end{bmatrix}^{n+1} = \begin{bmatrix} \mathbf{r}_1 \\ \mathbf{r}_2 \\ \mathbf{r}_3 \end{bmatrix}^{n}$$

Very large, ~ (10^7 x 10^7) non-diagonally dominant, non-symmetric, ill-conditioned sparse matrix (contains all MHD waves)

How best to solve this?

Preconditioned iterative method (Krylov subspace)

3 step physics-based preconditioner makes final iterative solve feasible and efficient

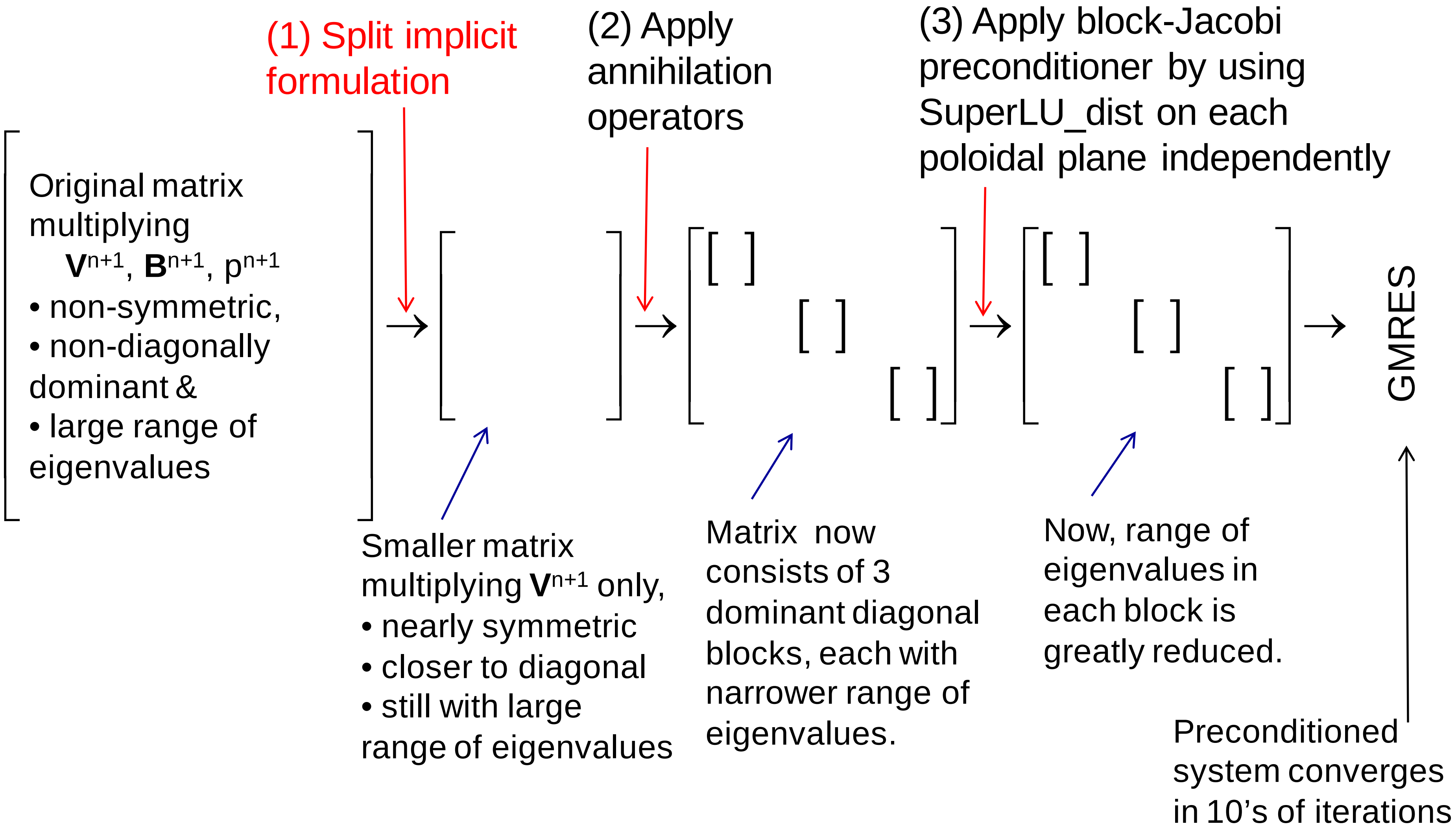

M3D-C^1 can be run with 1, 2, or 3 velocity variables. Tracking the eigenvalues shows how they separate into 3 groups in a cylinder

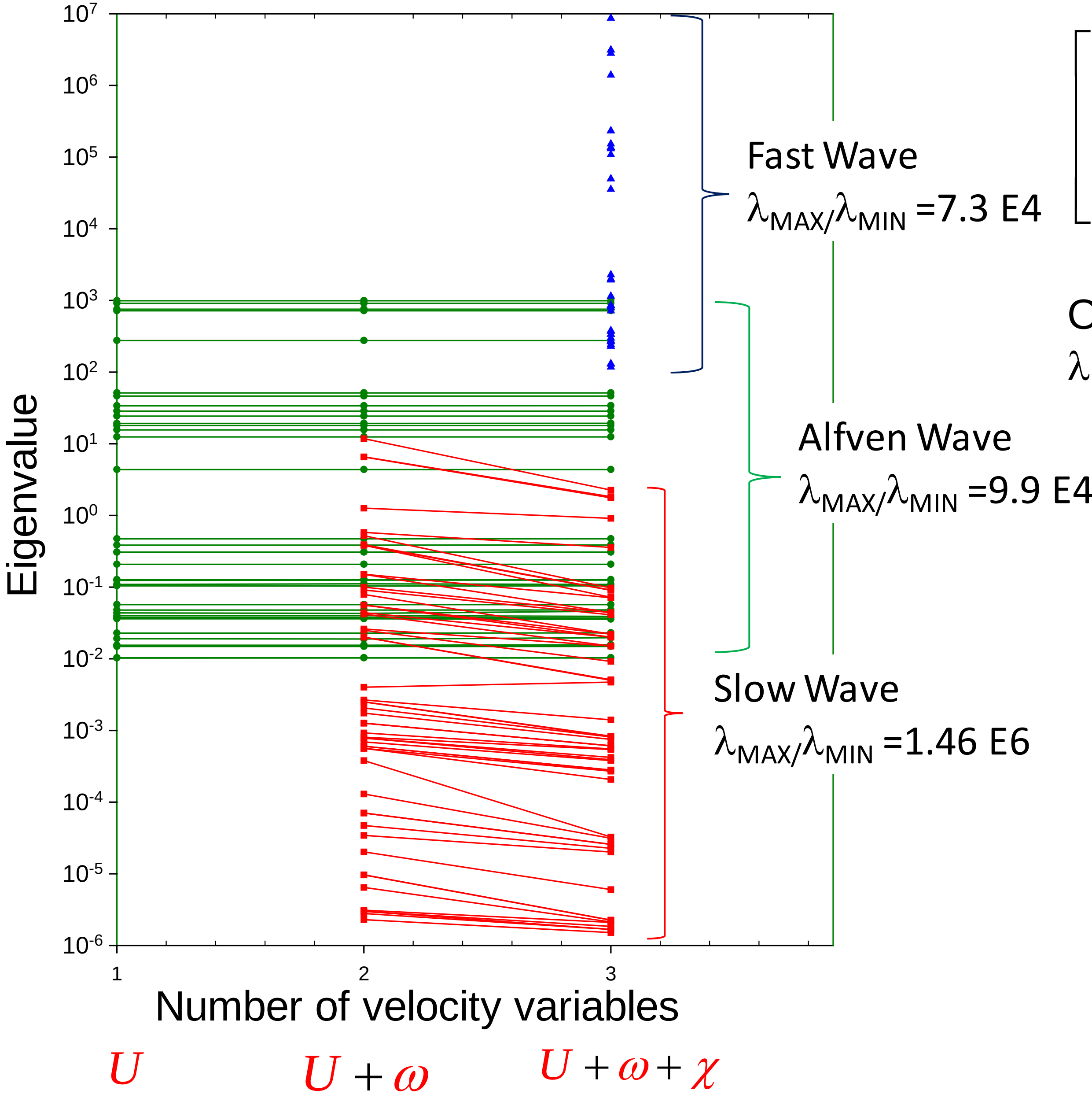

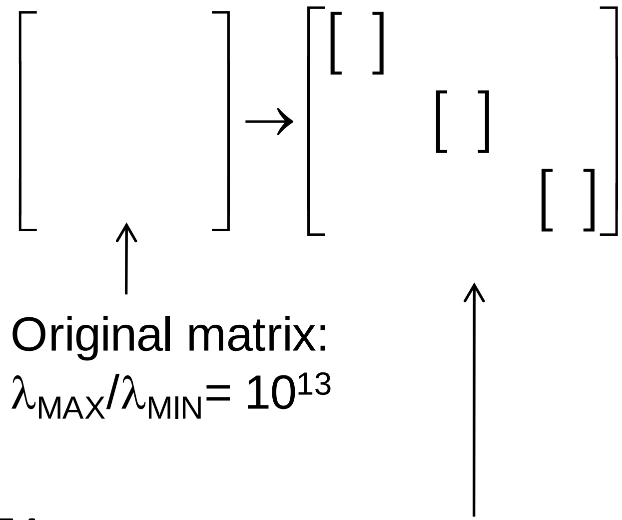

Original matrix: $\lambda_{MAX}/\lambda_{MIN} = 10^{13}$

Annihilation operators split this into 3 loosely connected matrices, each with a condition number much less than original matrix

$$\rho(A) \equiv \frac{|\lambda|_{max}}{|\lambda|_{min}} \quad 10^{15} \rightarrow 30!!!$$

Eigenvalues of A=3 3D Matrix **Before** and **After** Preconditioning

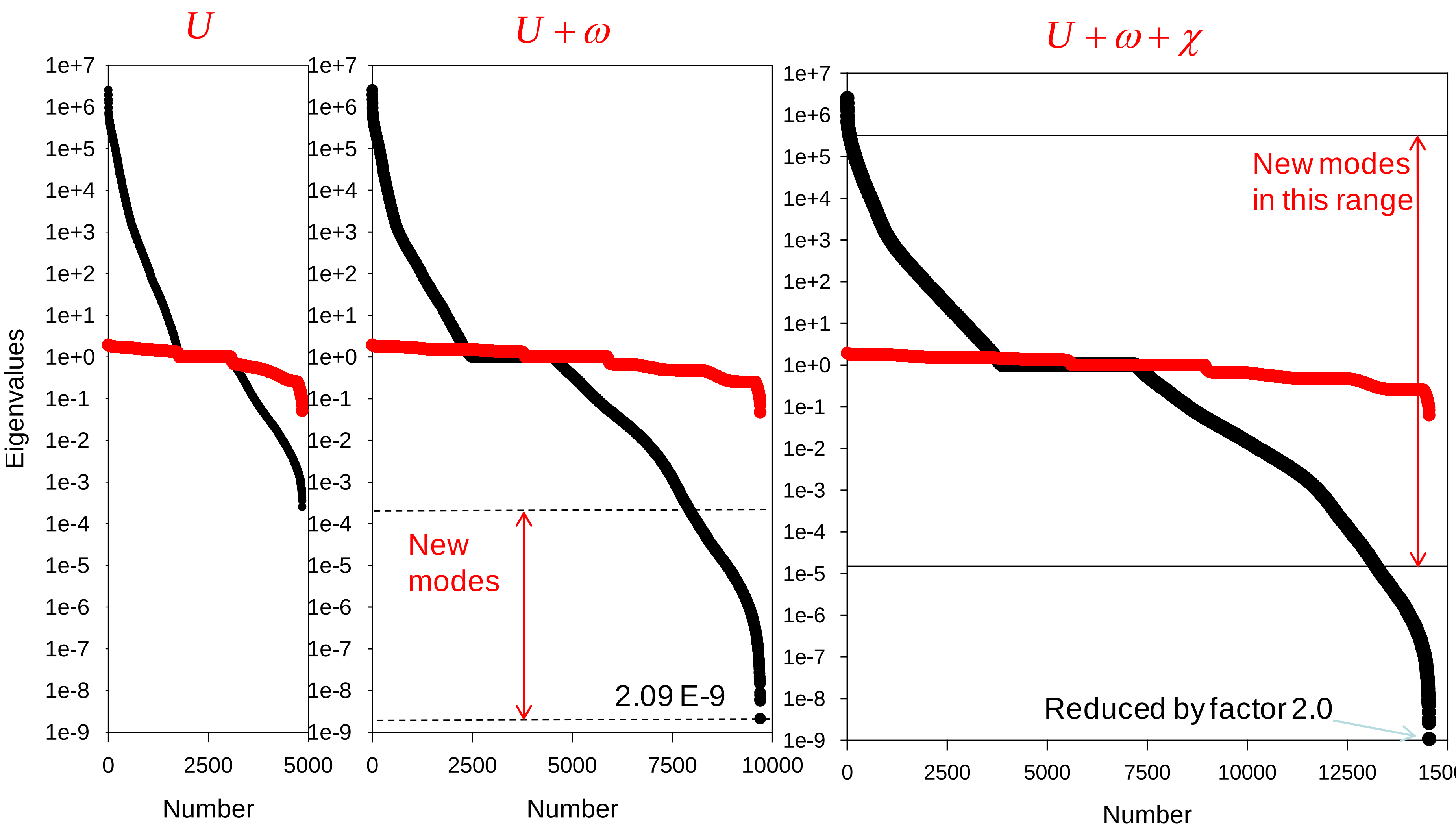

Parallel Scaling Studies have been performed from 96 to 12288 p

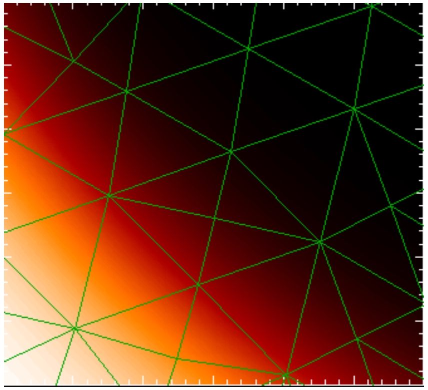

.08

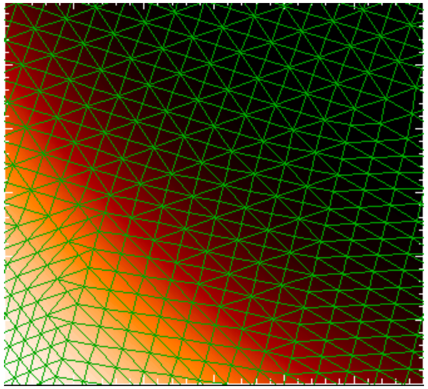

.02

Triangle linear dimension varied by factor of 4

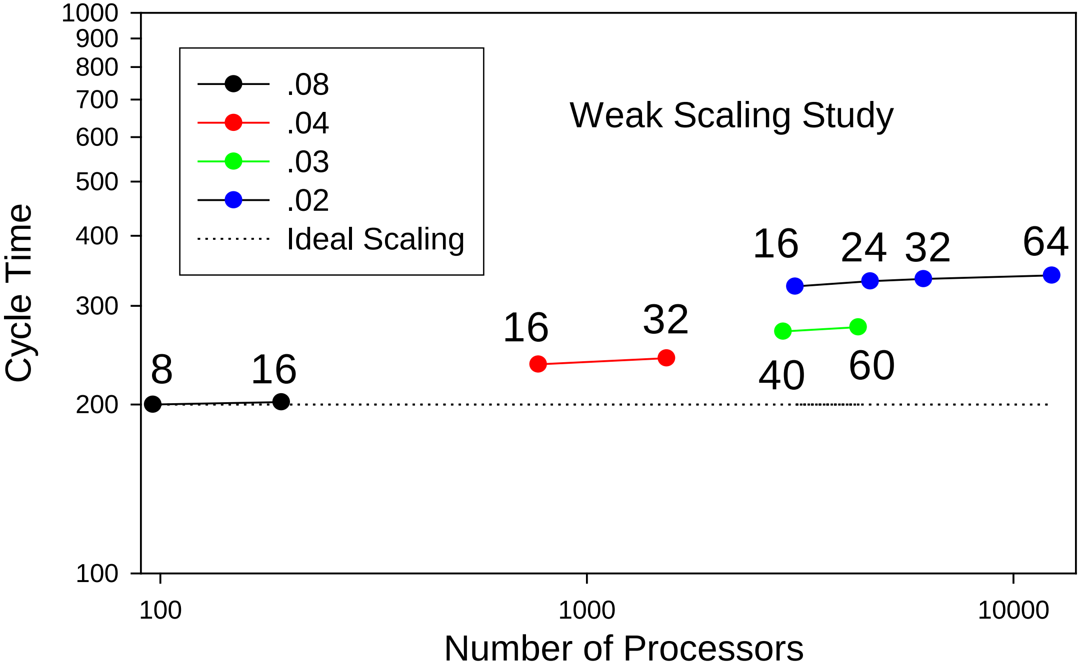

Number of toroidal planes varied from 8 to 64

Time increased by 1.7 as # of zones increased by 130

Extensive benchmarking for ideal, resistive, and two fluid modes

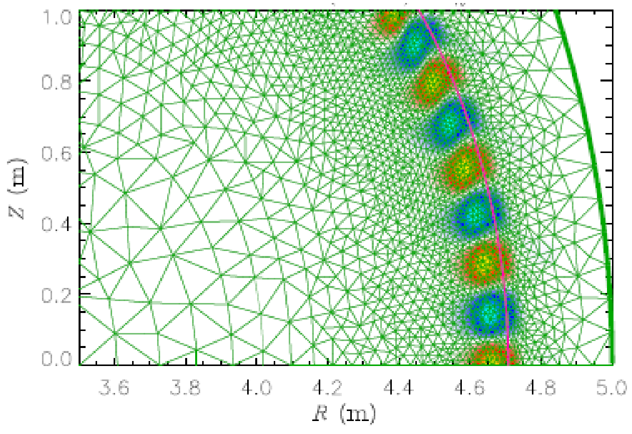

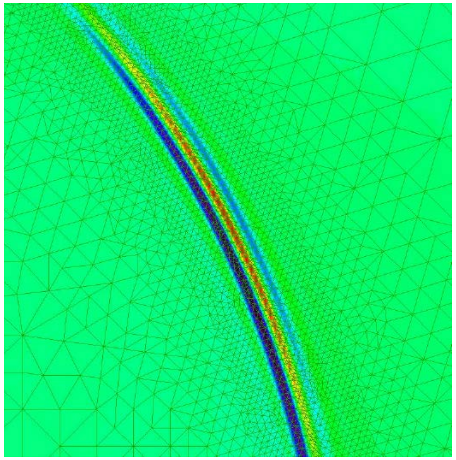

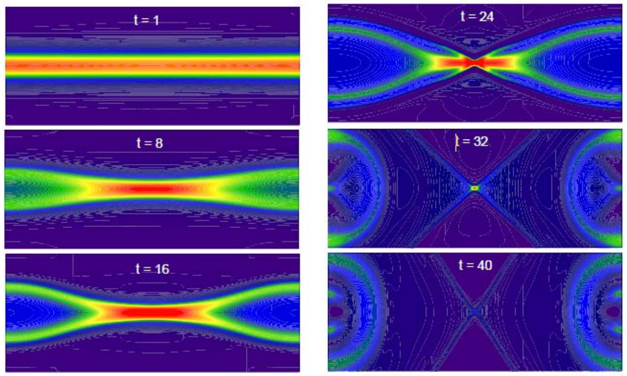

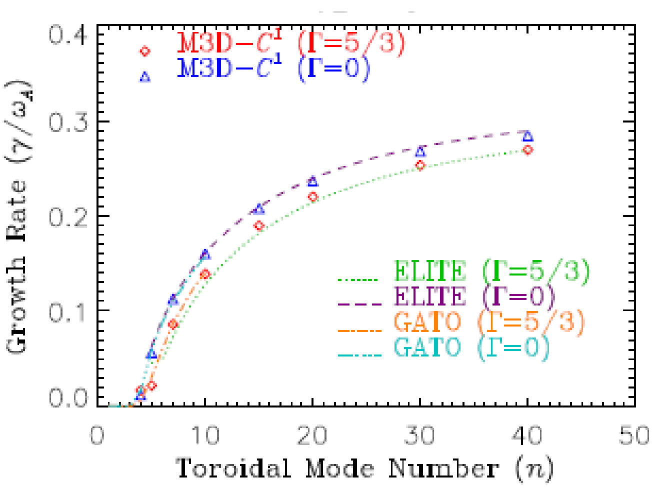

Ideal MHD

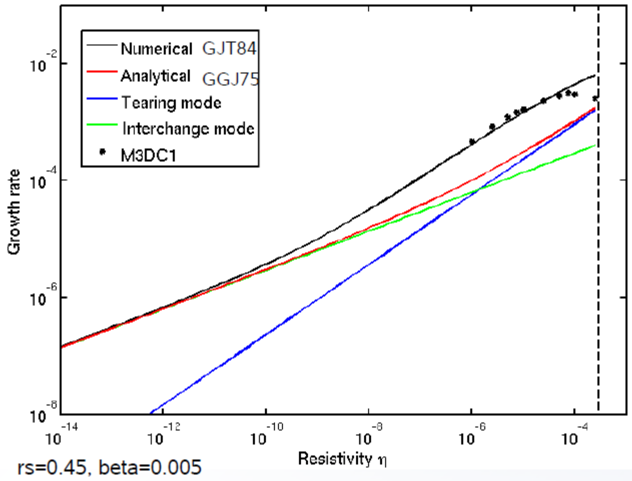

Resistive MHD

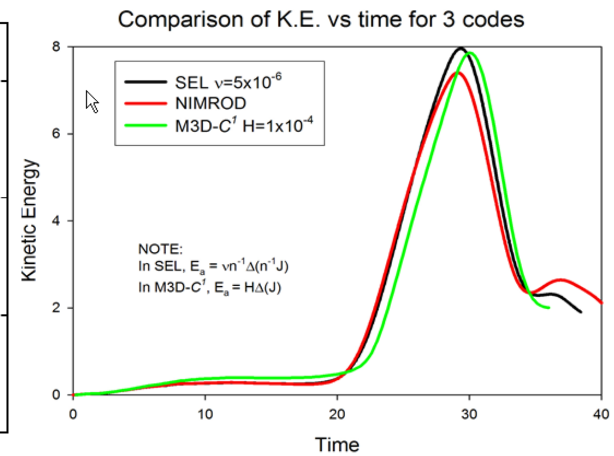

2-Fluid Reconnection

NSTX pressure driven modes with $q_0 \geq 1$

Series of geqdsk equilibrium for shot 124379 generated by S. Gerhardt for 2011 Breslau, et al NF paper.

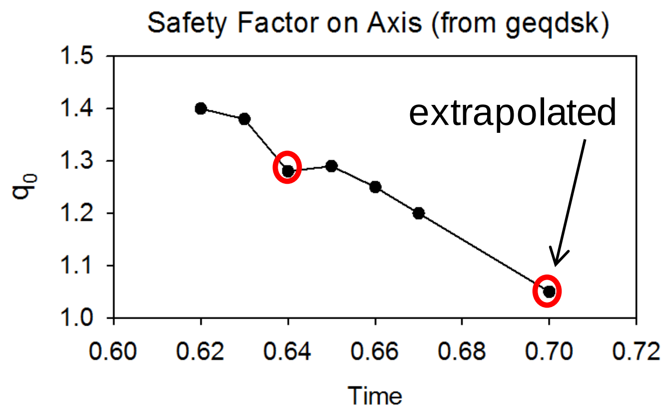

$$\beta_P \simeq 0.8$$

$$\beta_T \simeq 7+\%$$

$$I_P \simeq 1\,MA$$

Midplane values →

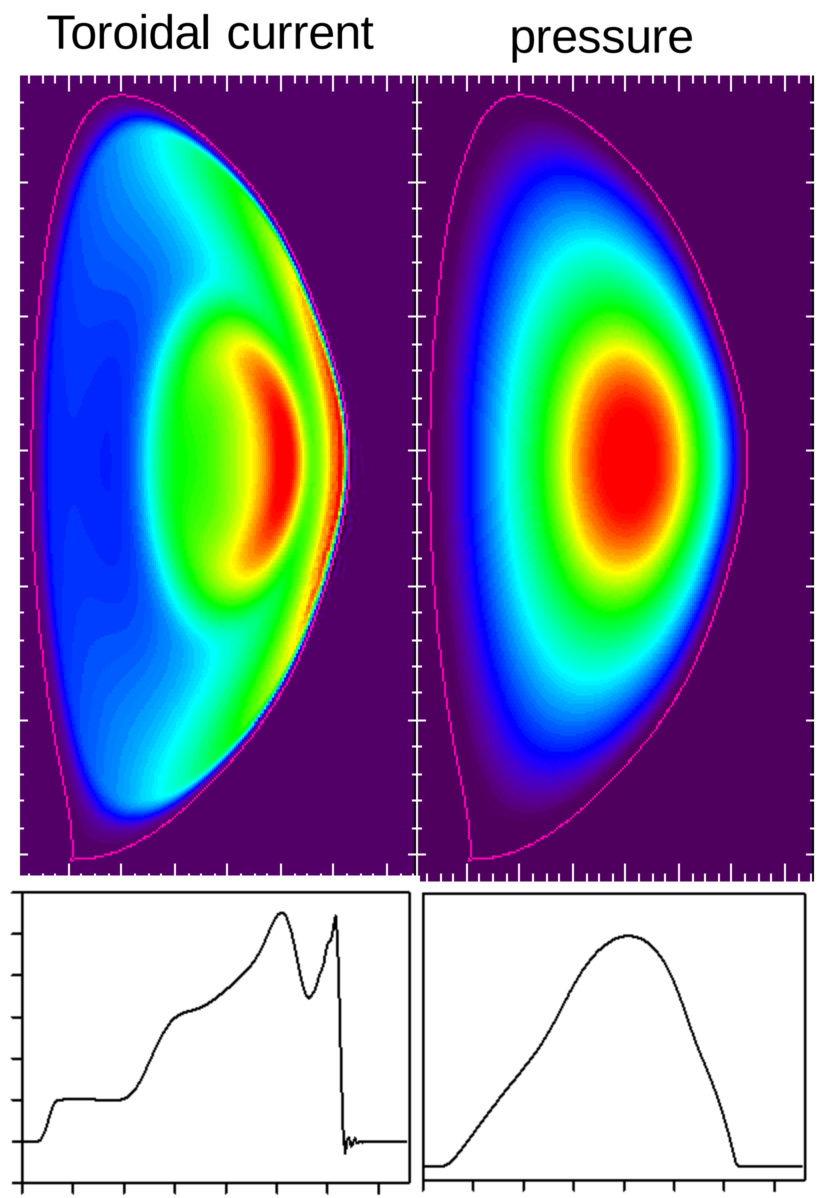

NSTX shot 124379 time 0.640
TF scaled by 0.9 so q_0=1.17

convergence studies for linear regime of nonlinear code

M3D-*C*[1] growth rate vs number of toroidal elements

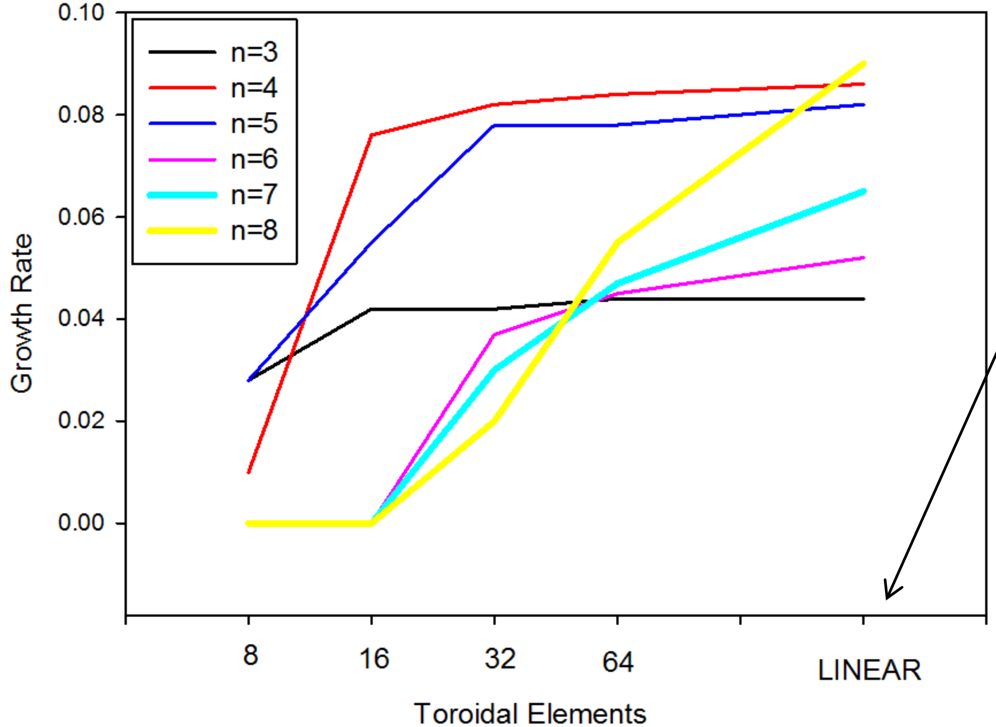

LINEAR result uses same code, but assumes φ dependence *exp(inφ)*, everything is complex, non-linear terms are not included

This scaled equilibrium was above the beta limit and unstable to many linear (interchange) modes with n>1.

The nonlinear code is ***converging from below*** to the linear result, which is essential for numerical stability in these cases.

Possible mechanism for soft beta limit

Shot 124379

Time .640

$q_0 = 1.28$

No toroidal rotation

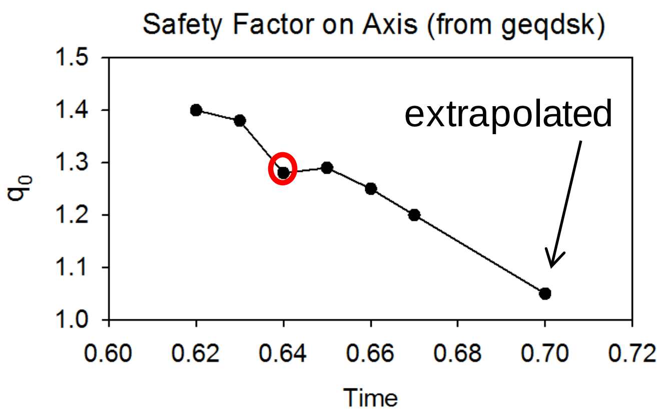

Initially, only n=3 is unstable

All modes saturate with K.E. decreasing with time

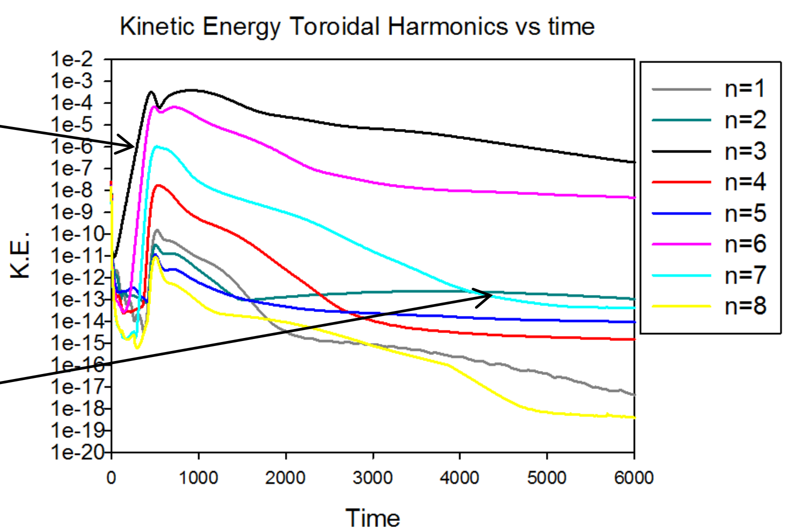

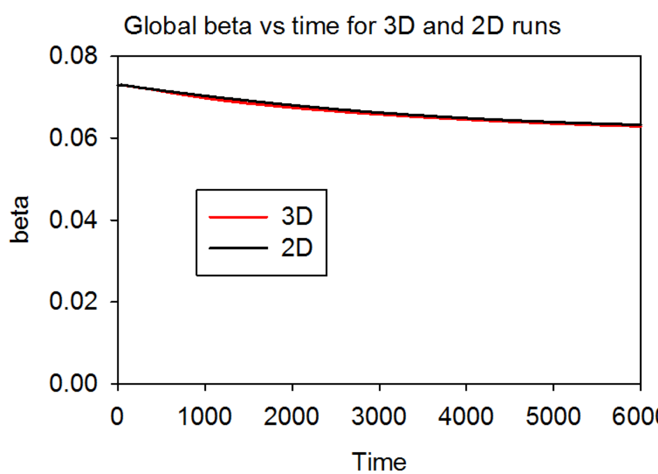

β decreases slightly in time, but no more than in an 2D run with same transport model

Soft beta limit

$q_0 = 1.28$

Poincare plots →

Surfaces deform, become stochastic, & completely heal.

ΔTe →

First pure n=3, then nonlinear, finally axisymmetric annulus

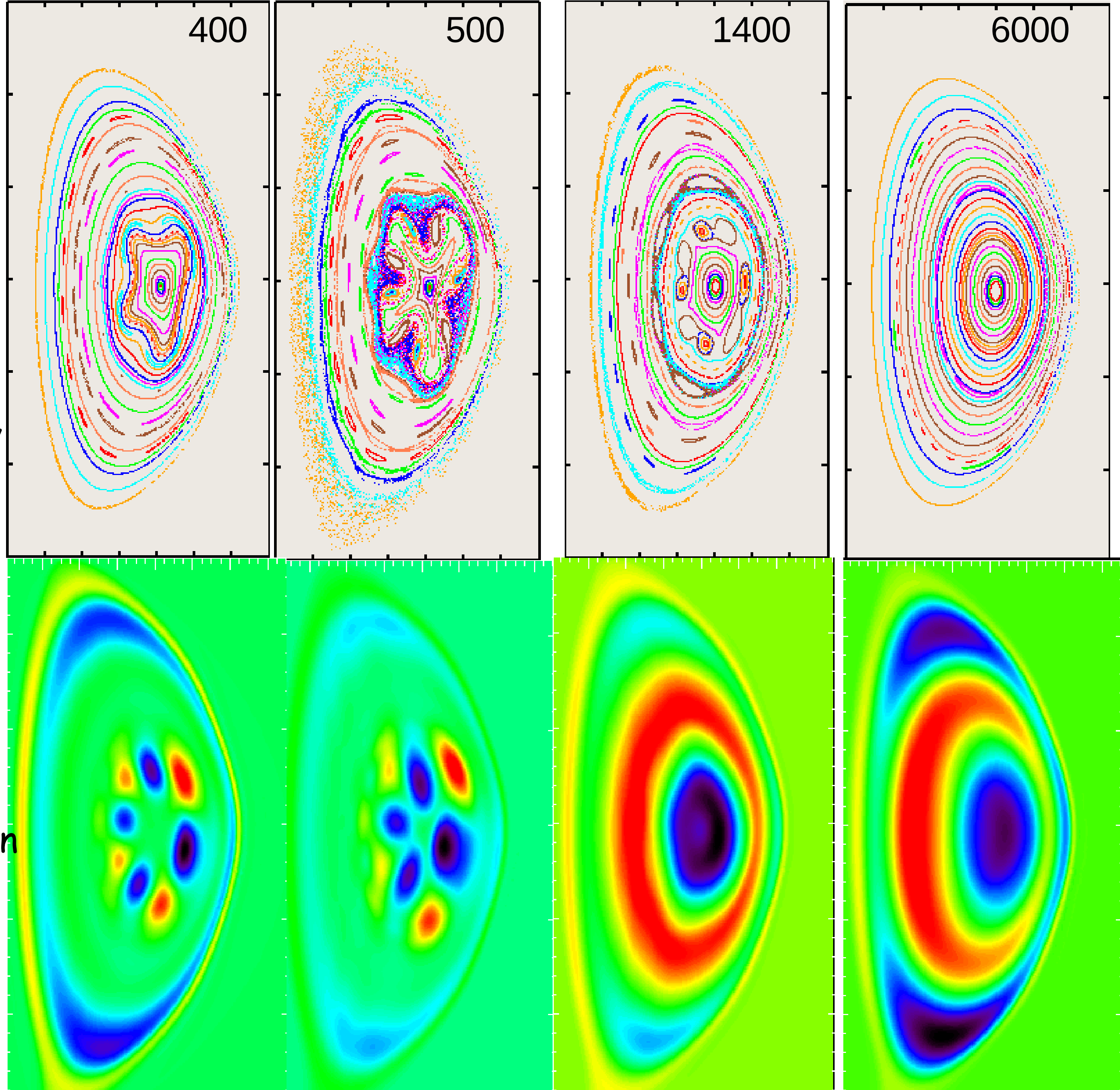

Job33

soft beta limit -- continued

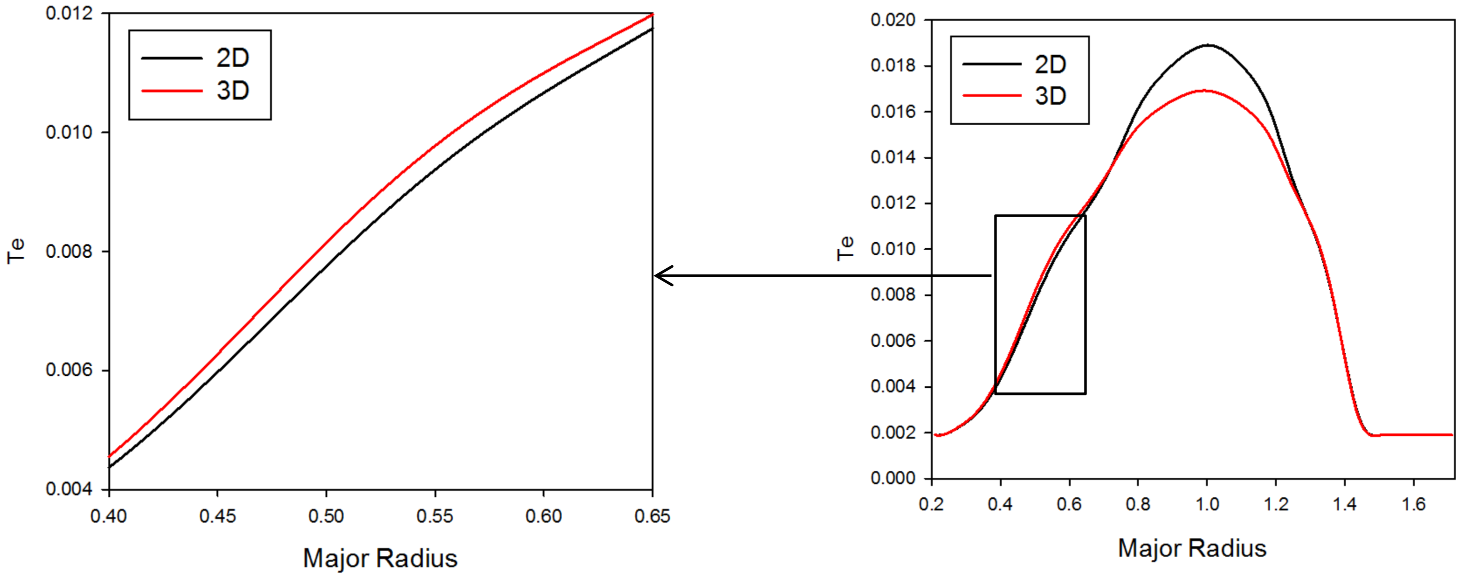

- Comparison of 3D run at t=6000 with 2D run with identical transport coeffs. shows thermal energy has been redistributed.

- Central Te differs by 10%, beta differs by only 0.6 %

dependence on heating source

- Previous run had beta decreasing in time, even in 2D case, because there was no heating source (except Ohmic).

- Now add *neutral beam source* to keep beta constant and to drive sheared toroidal rotation

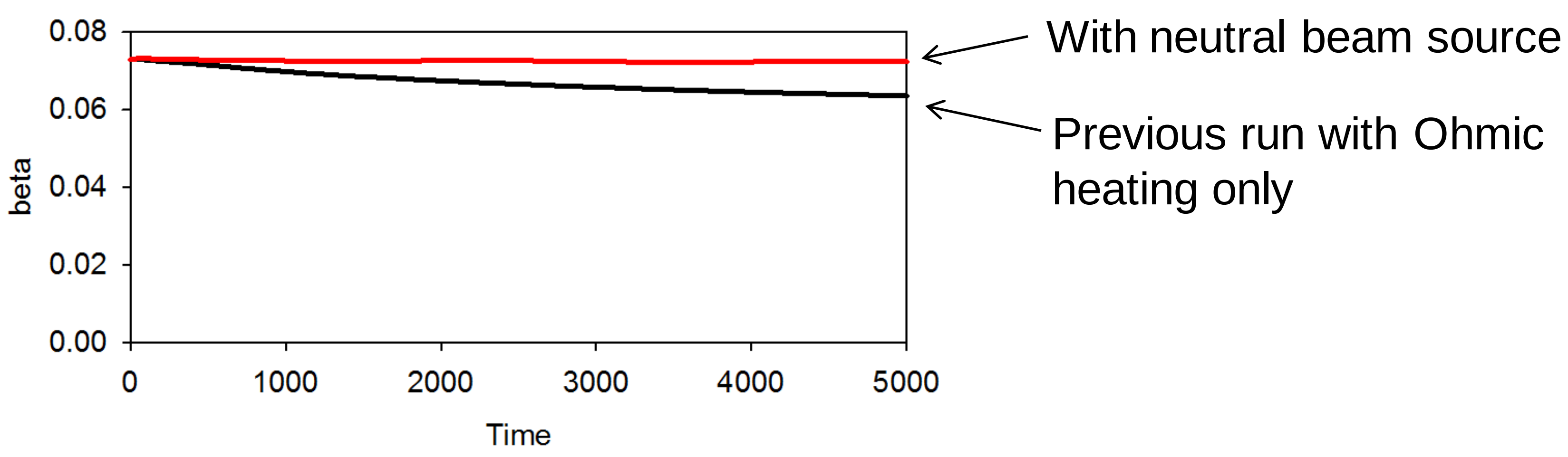

dependence on heating source–cont.

Ohmic heating only

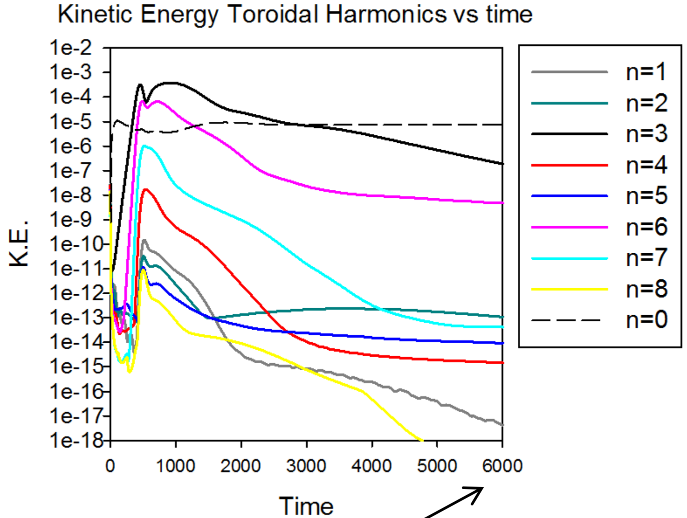

With neutral beam source

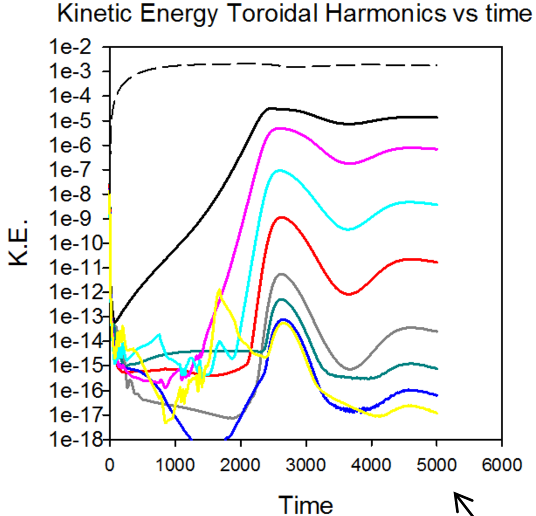

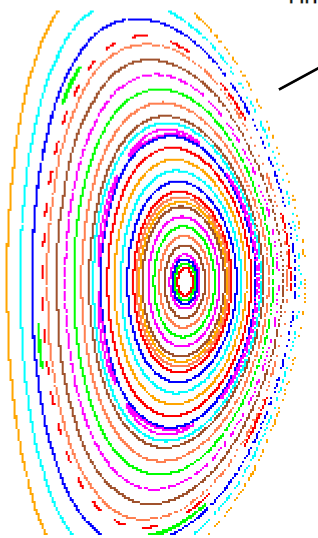

With heating and momentum source: (constant beta and sheared rotation)

- Initial linear growth of n=3 mode much slower
- n=3 and higher harmonics do not decay away: surfaces distort

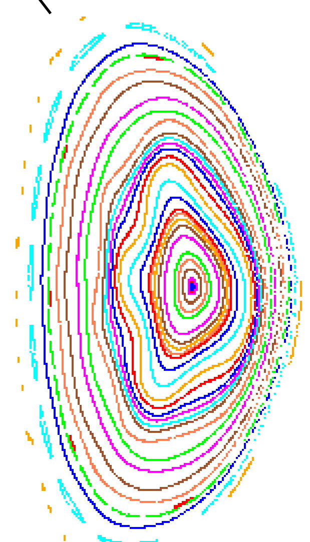

effect of increasing (decreasing) heating

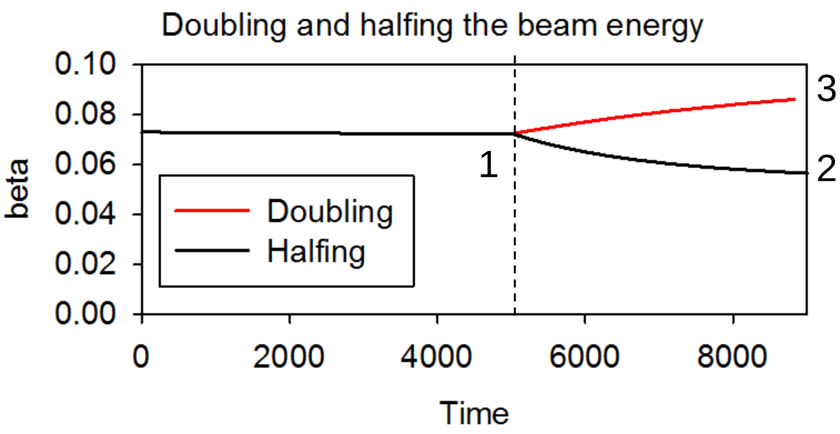

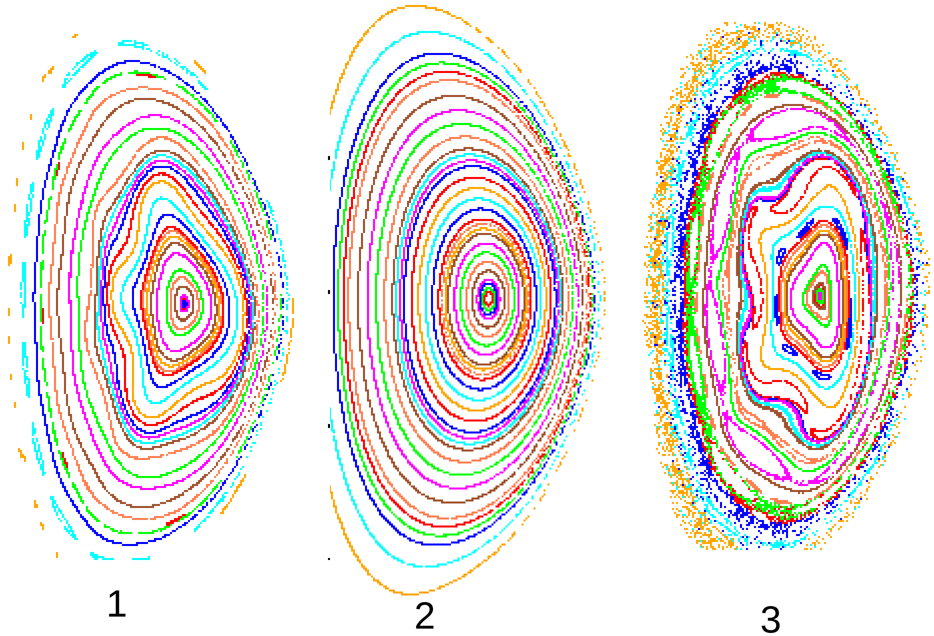

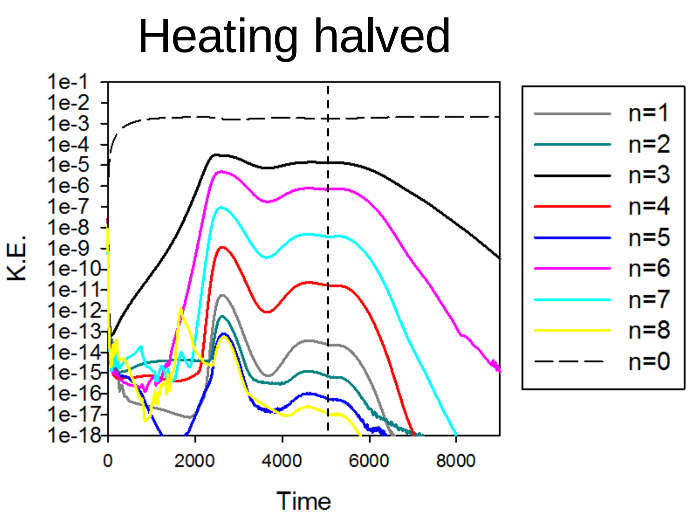

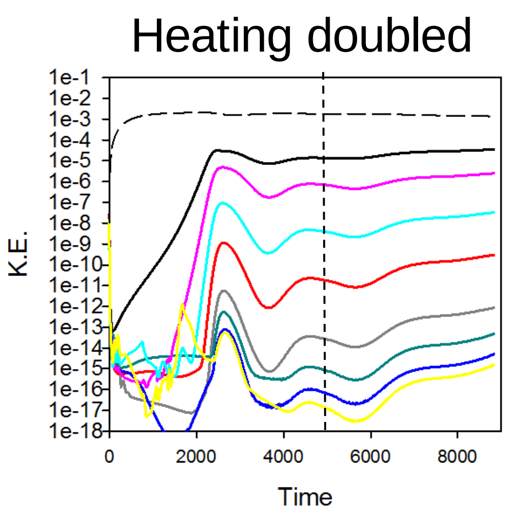

- With heating *reduced*, plasma returns to an axi-symmetric state (2)
- With heating *increased*, surfaces become more distorted, but still exhibits confinement (3)

effect of increasing (decreasing) heating

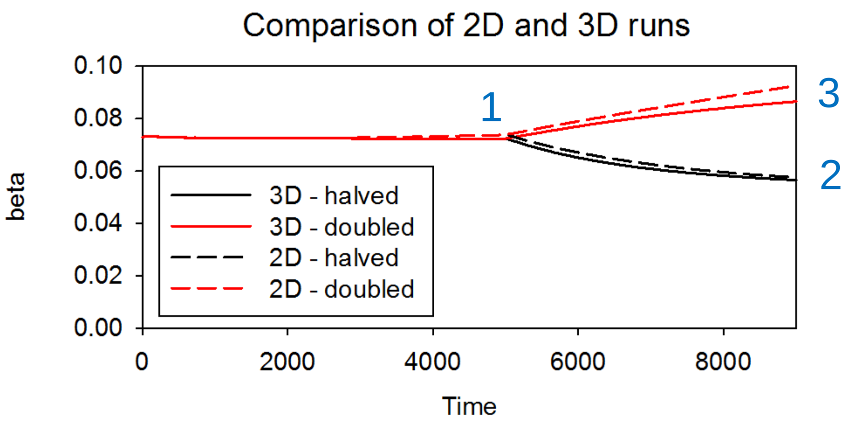

- at low heating power, Te profiles from 2D and 3D agree
- at higher heating powers, they differ considerably

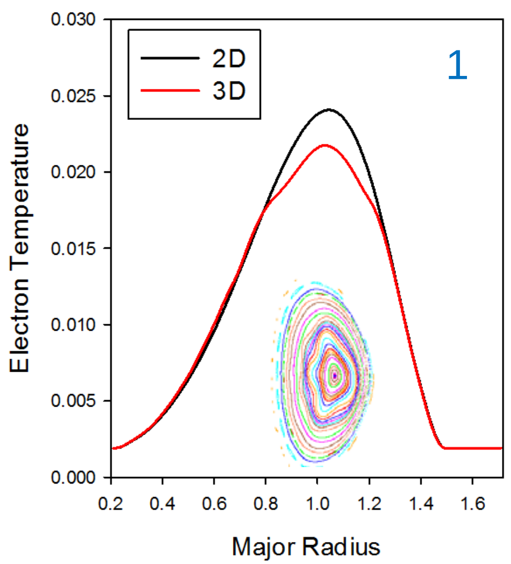

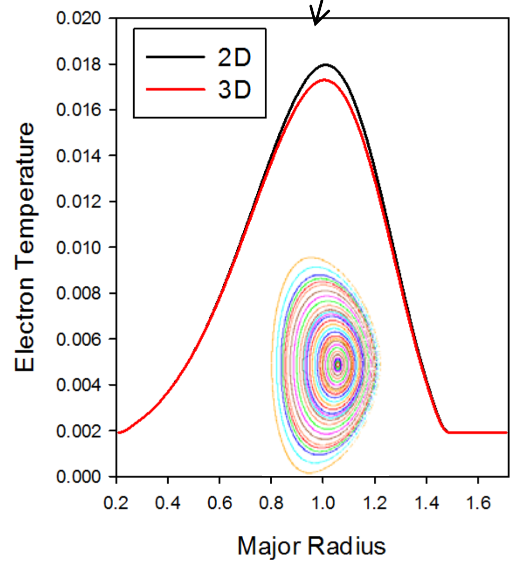

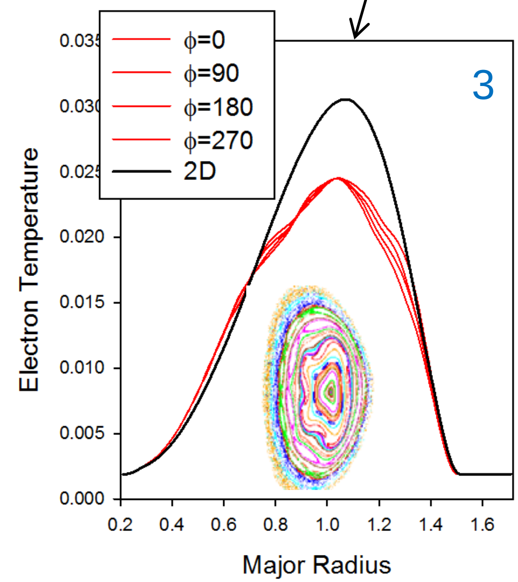

importance of sheared rotation

With heating and momentum input (sheared rotation)

With heating only (no rotation)

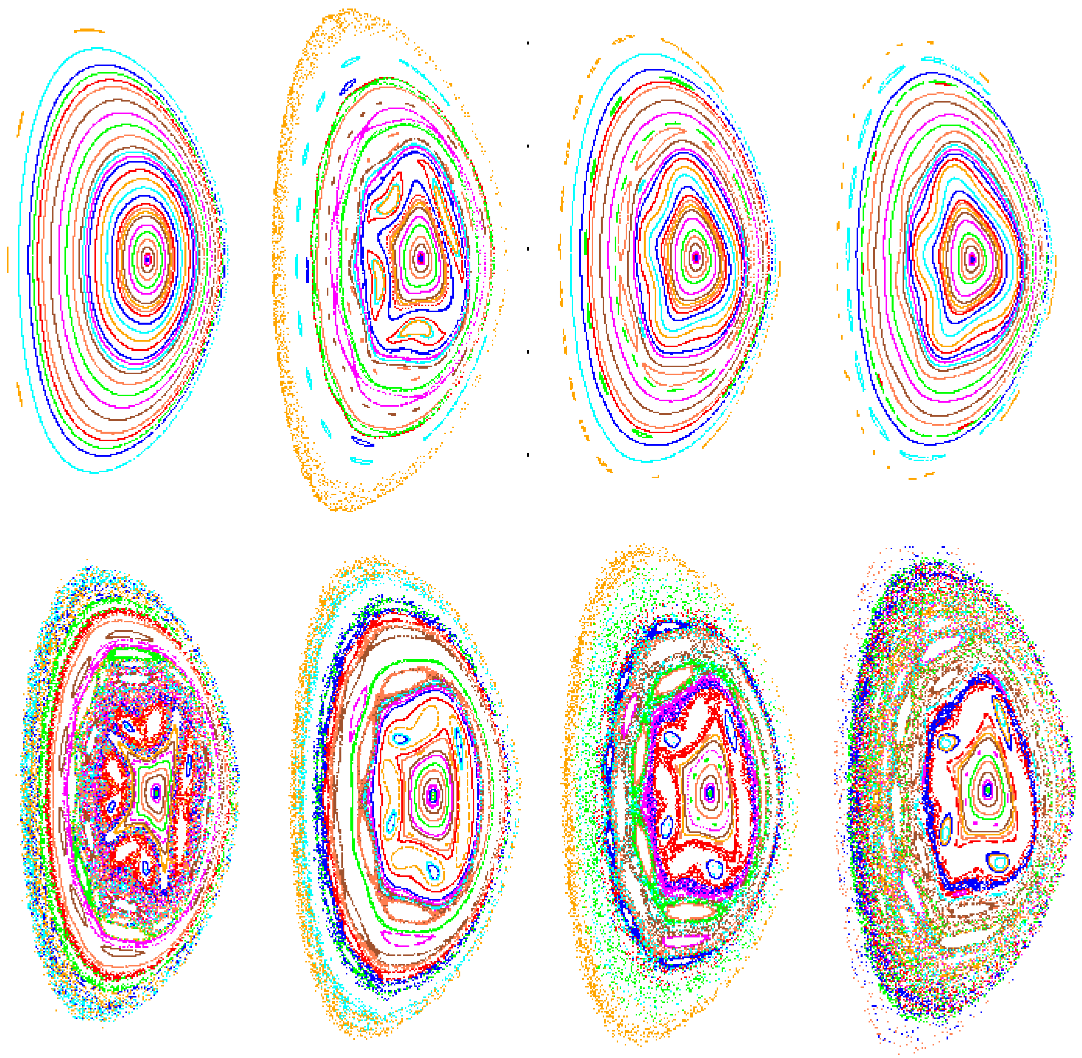

t=2000 t=3000 t=4000 t=5000

equilibrium with lower q_0 shows thermal collapse

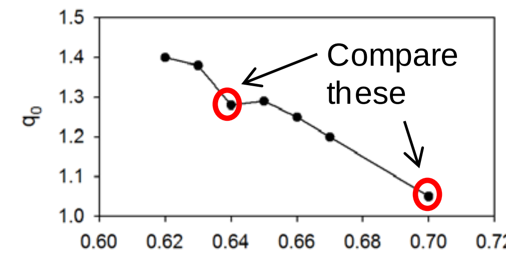

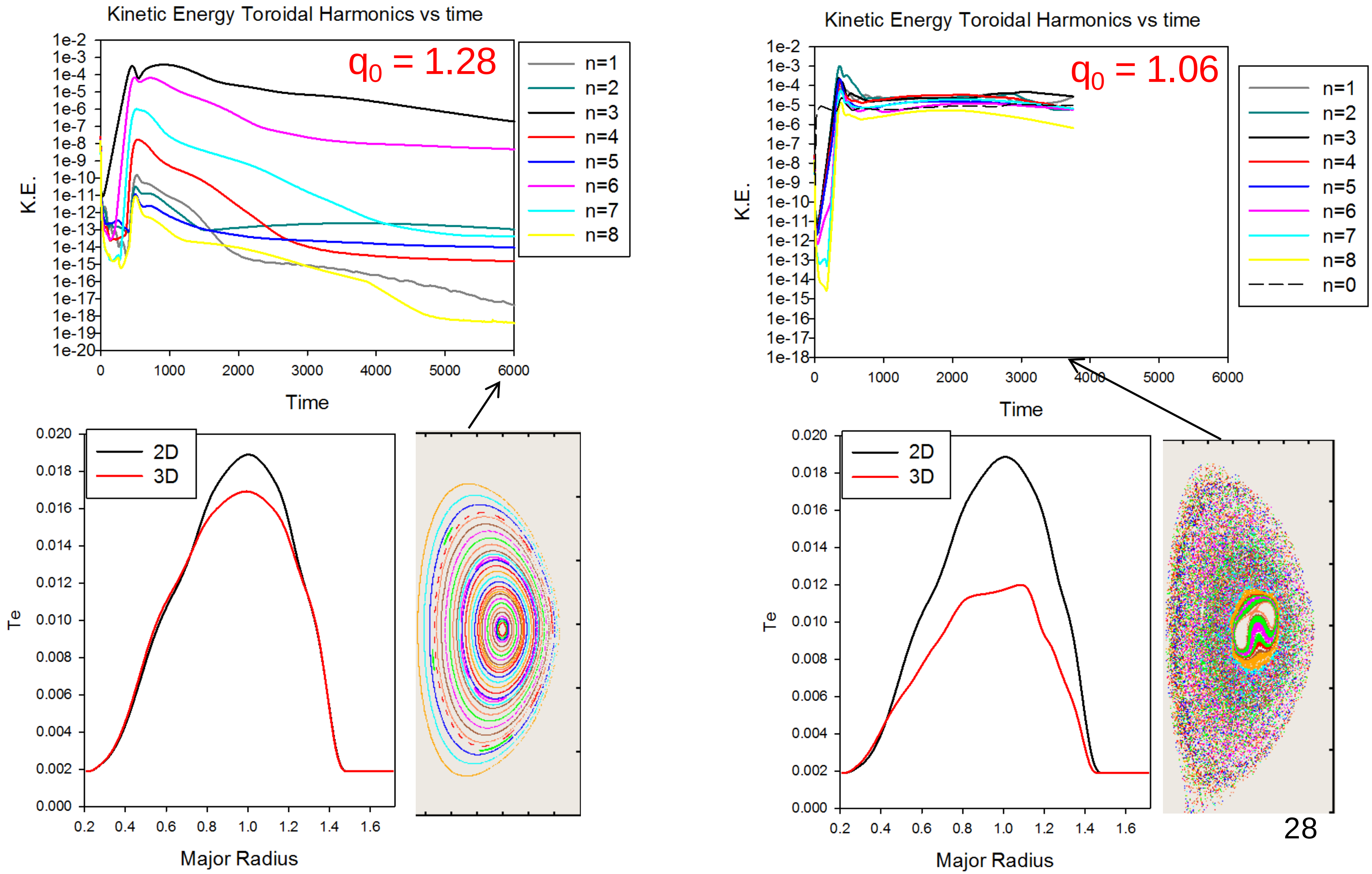

numerical convergence study

Original constant β run

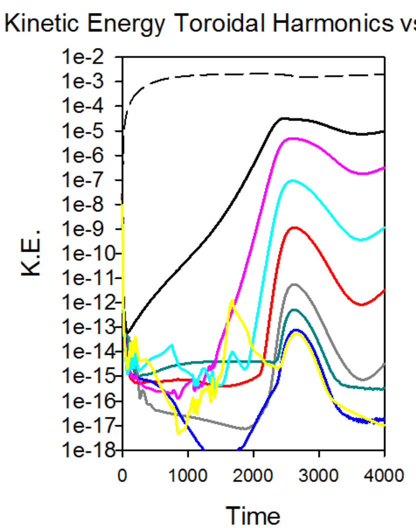

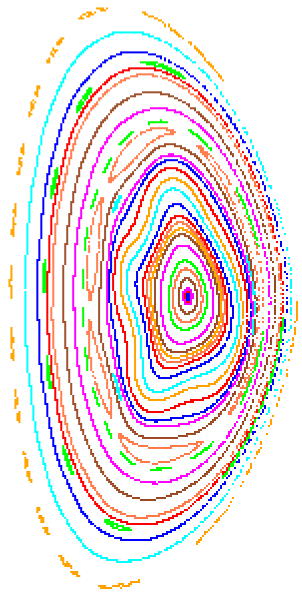

With double the poloidal zones

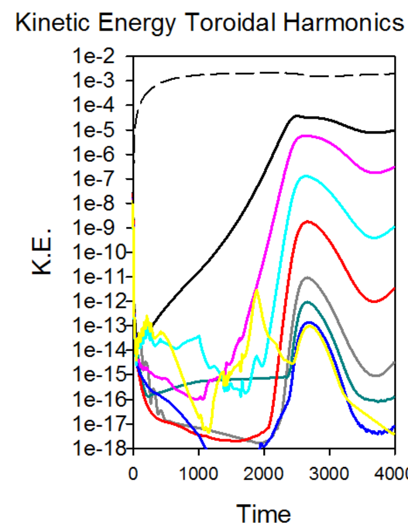

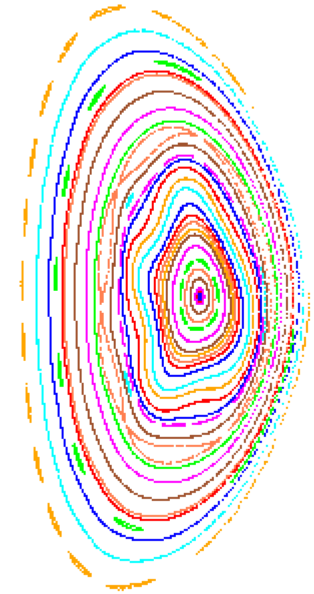

Sawtooth Studies-1:

Specify transport model and loop voltage and let system evolve.

Typical result: 1st sawtooth event depends on initial conditions.
After many events, system reaches steady-state or periodic behavior

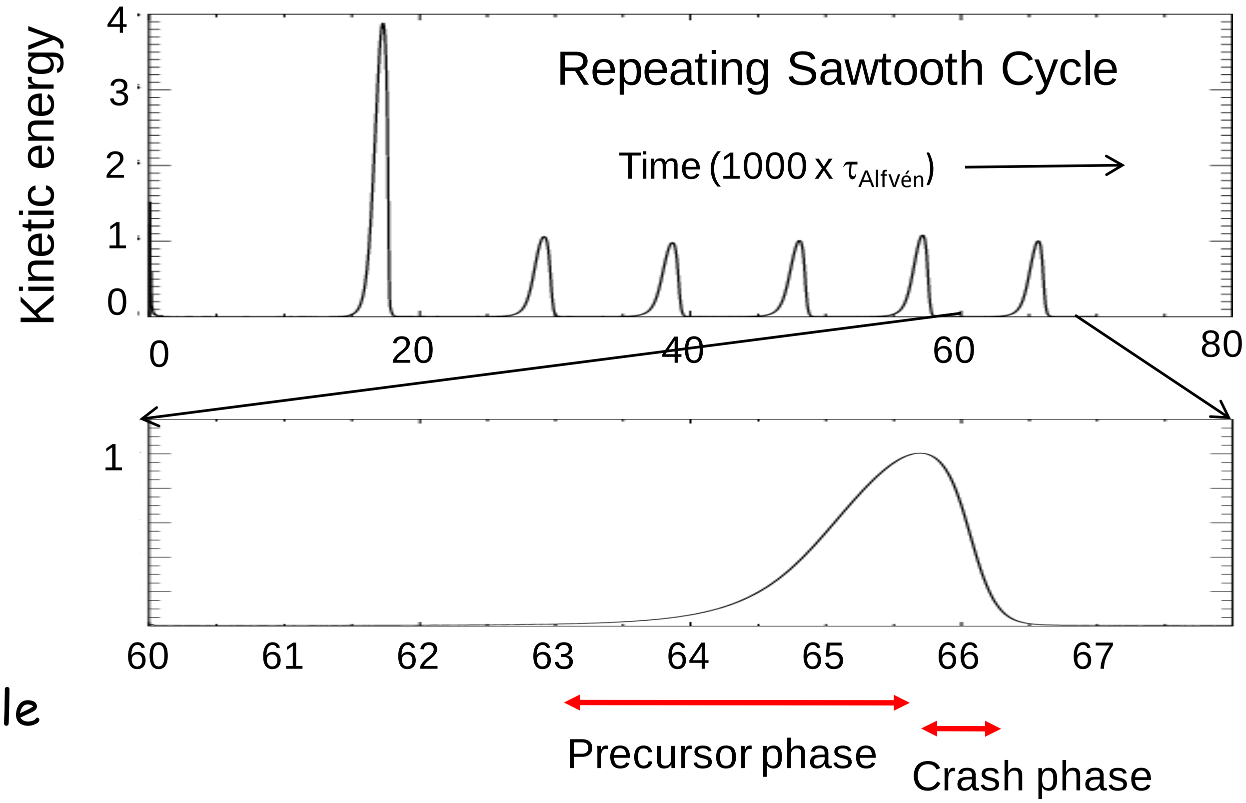

Repeating sawtooth cycle

CMOD

Sawtooth Studies-2:

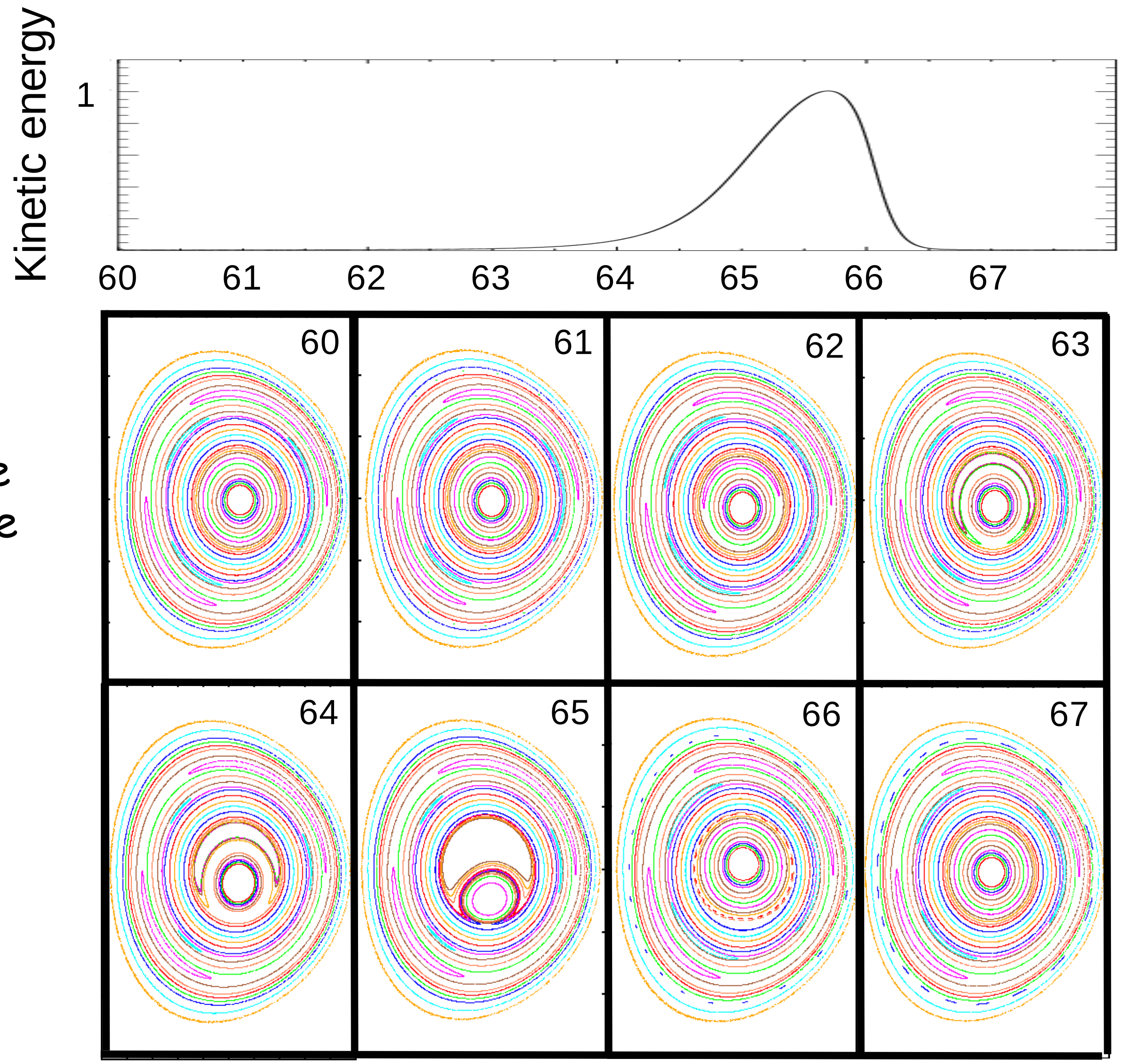

Poincare plots during a single sawtooth cycle

CMOD

$$\mathbf{V} = R^2 \nabla U \times \nabla \phi + R^2 \omega \nabla \phi + \frac{1}{R^2} \nabla_{\perp} \chi$$

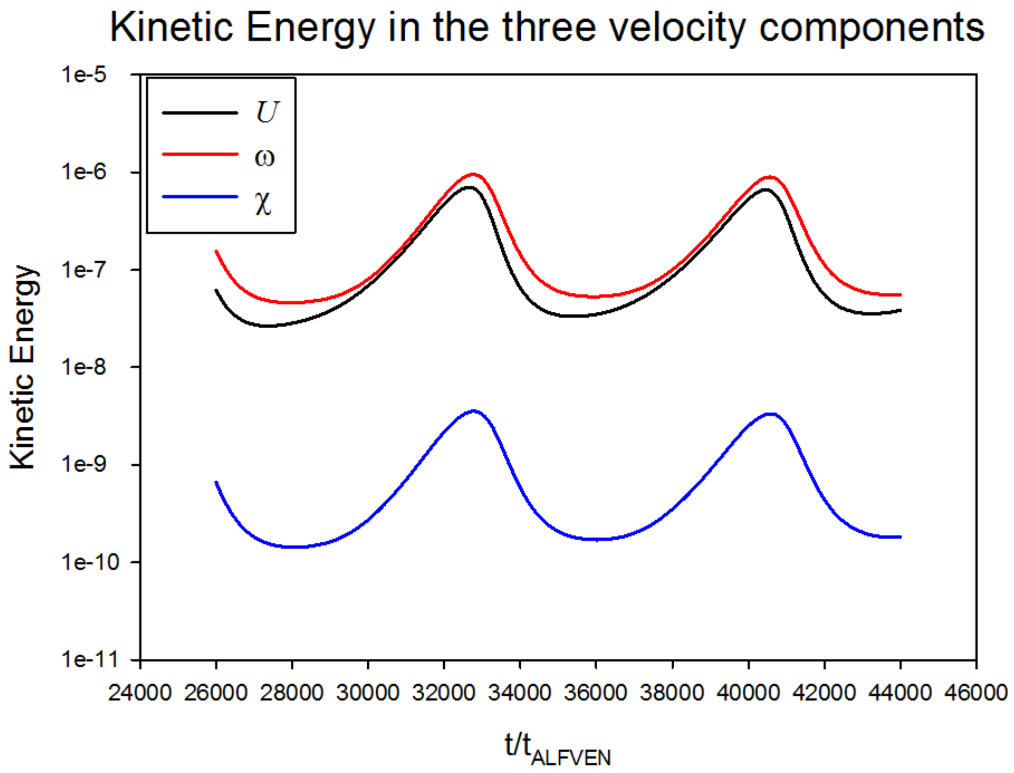

The poloidal velocity decomposition used in M3D-C^1 is very effective in capturing most of the poloidal flow in U.

Sawtooth Studies-3:

For other transport parameters (η,κ,μ), after an initial transient, system reaches stationary-state with flow with $q_0 \cong 1$

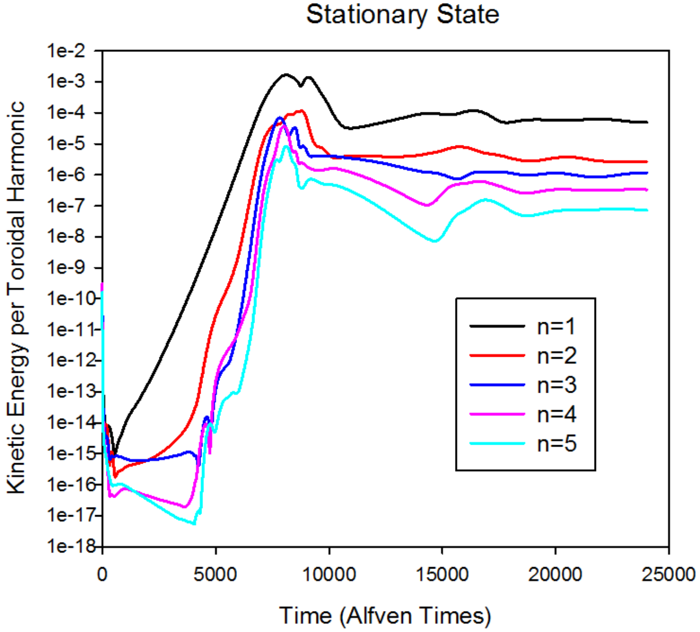

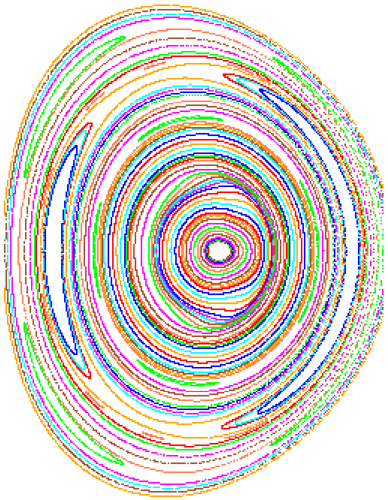

Poincare plot at final time

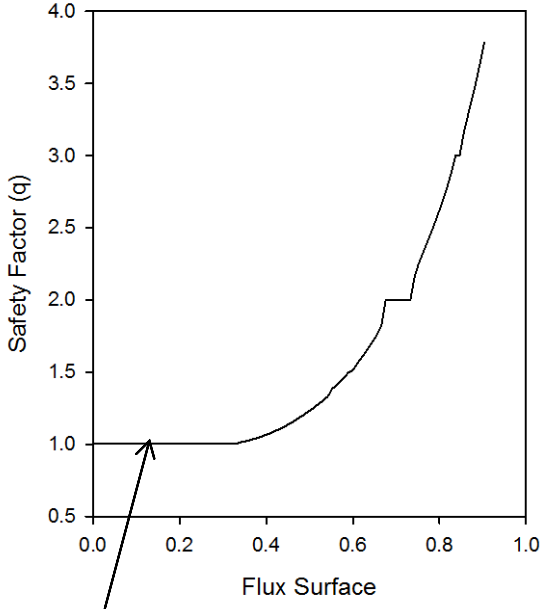

Note large region with $q = 1 + \varepsilon$

Sawtooth Studies-4:

Stationary state

Electron Temperature

Poloidal velocity stream function U

$$\mathbf{V} = R^2 \nabla U \times \nabla \phi$$

Toroidal angular velocity ω

$$\mathbf{V} = R^2 \omega \nabla \phi$$

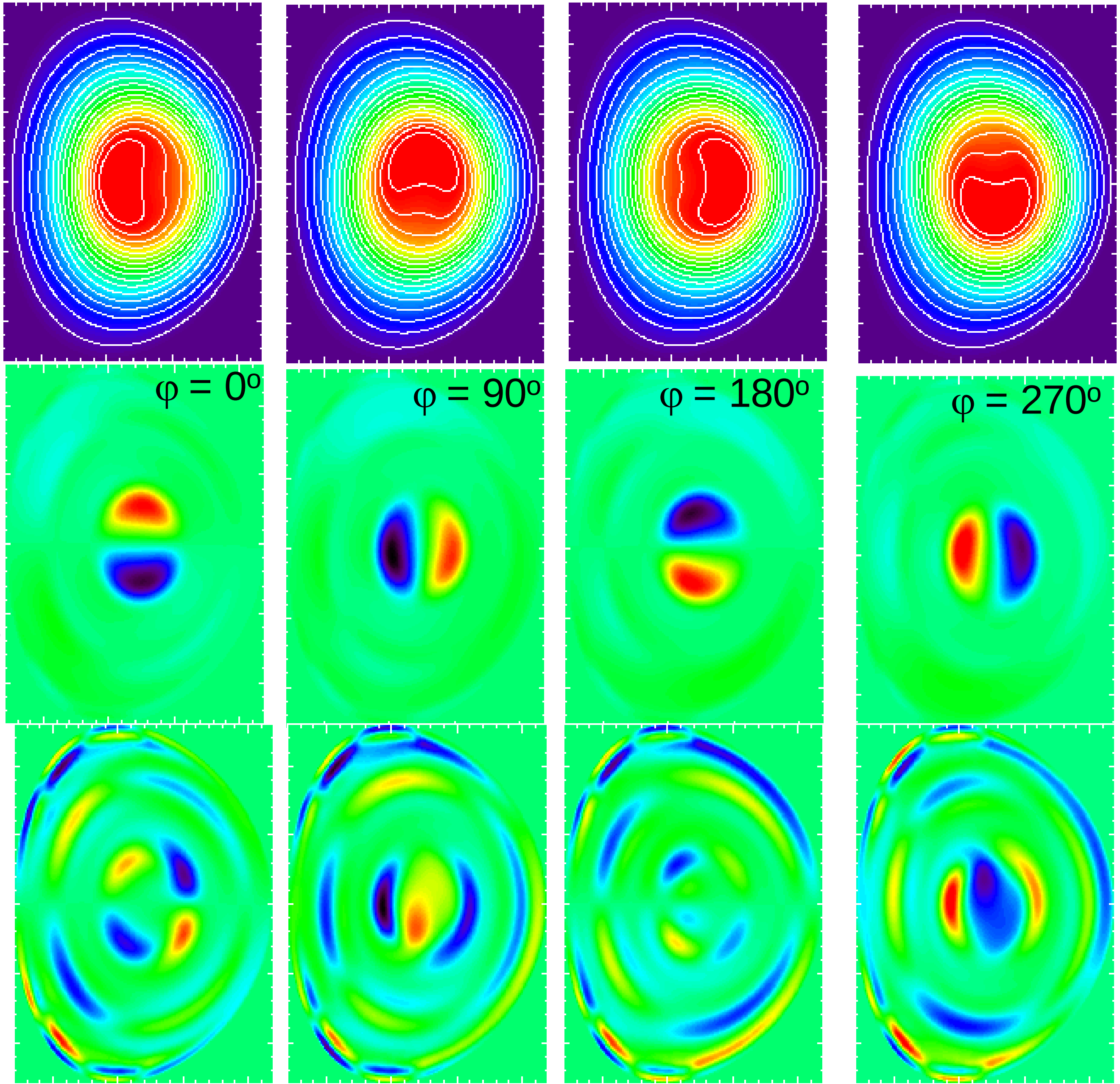

Sawtooth Studies-5:

Comparison of midplane profiles at different toroidal locations with profiles from an identical 2D run at the same time (same transport coefficients)

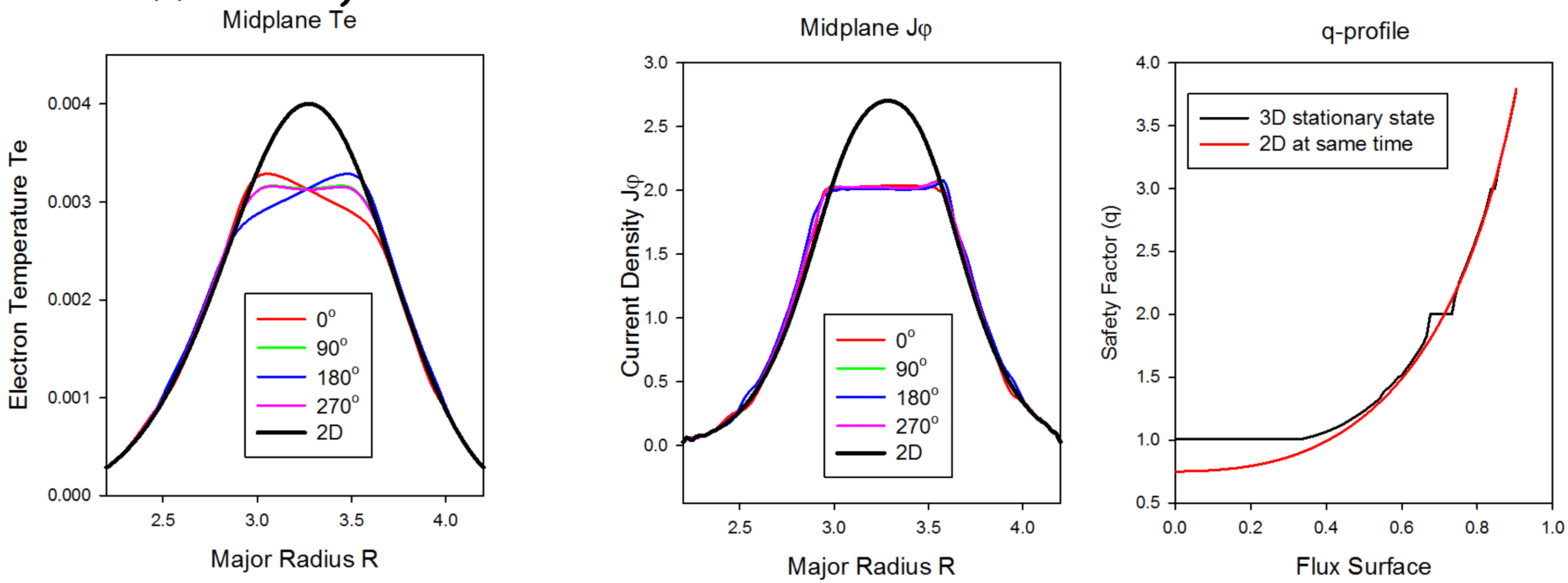

In 3D, the velocity generated from the instability at q = 1 acts to distort and flatten the Te profile and J profile, which keeps q pegged at $(1. + \varepsilon)$

New meshing routines being developed to include wall

The SCOREC group at RPI is developing new mesh routines that will include a capability for a resistive wall surrounding the plasma.

Each triangular element will belong to either the plasma region, the wall region, or the vacuum region.

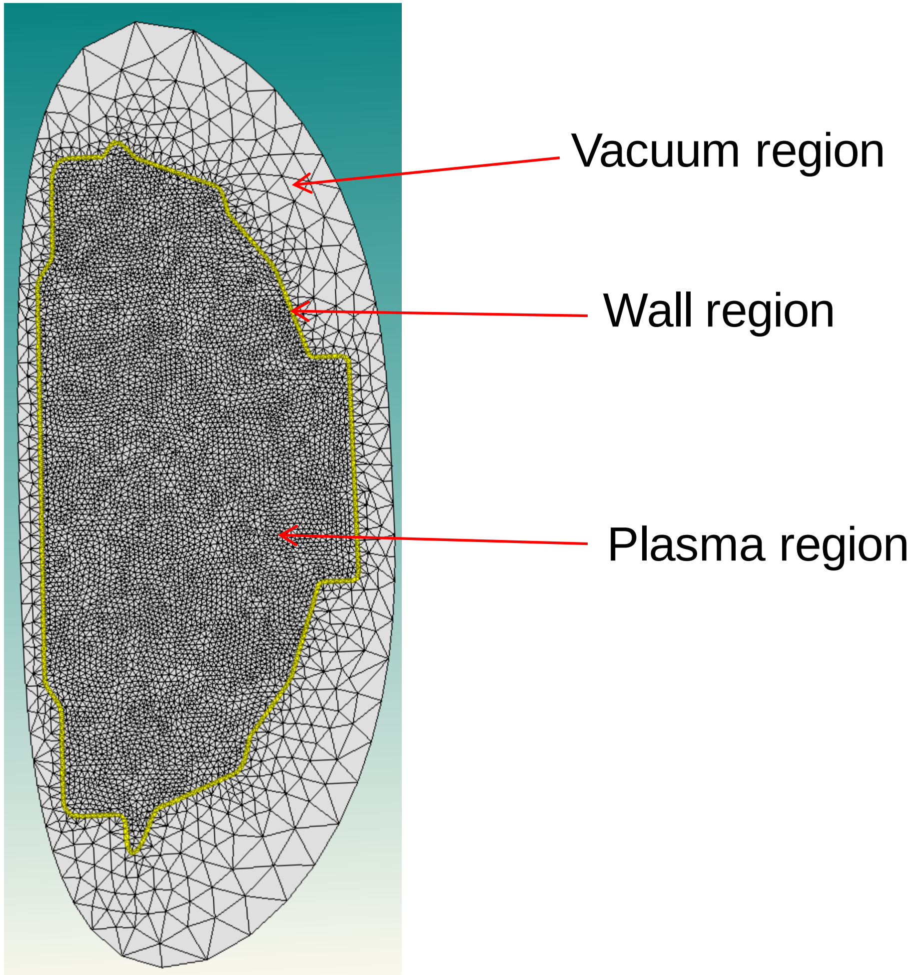

Inductive transfer of current to wall

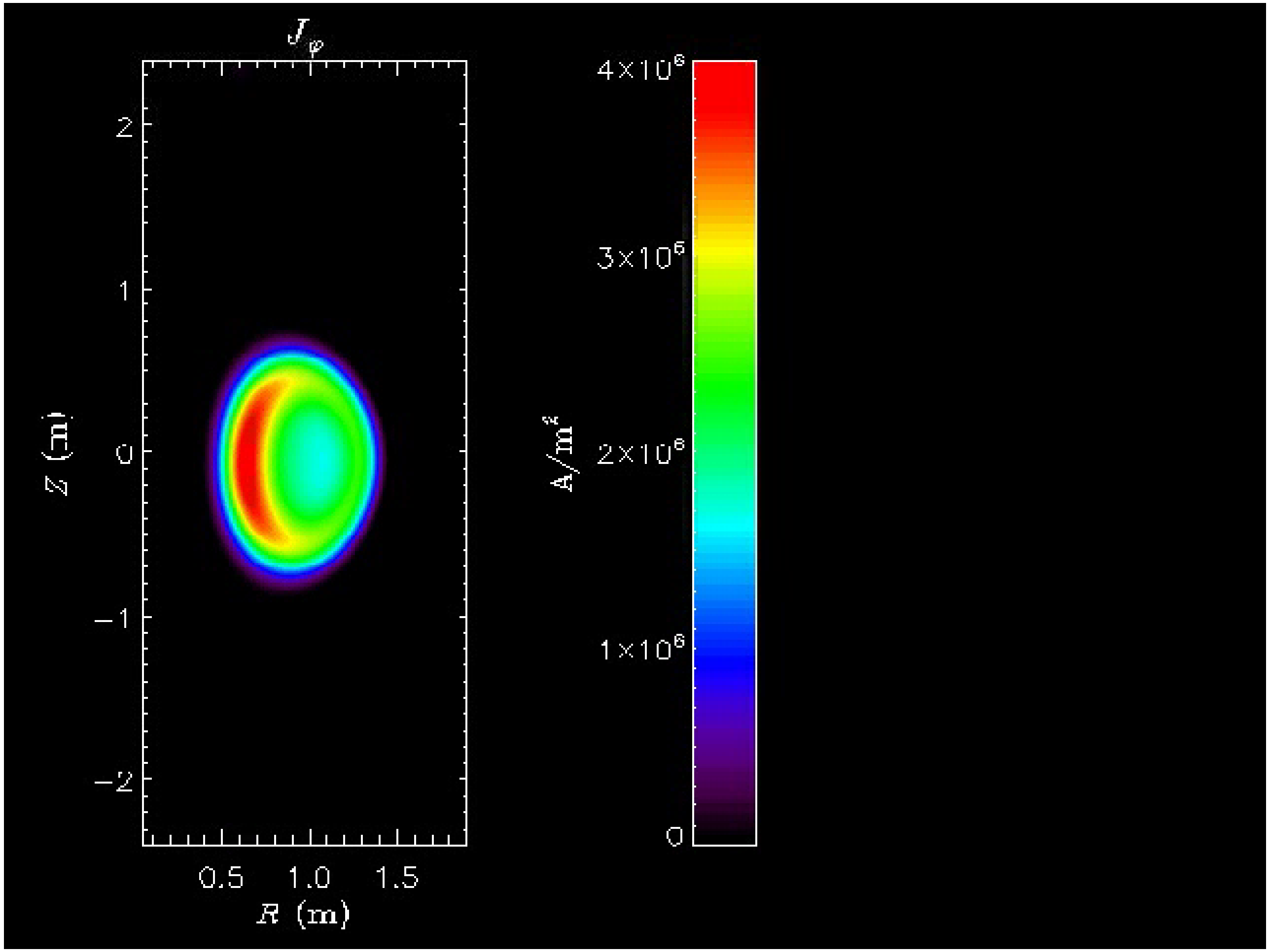

summary

- M3D-C^1 working nonlinearly in production mode
- Studying nonlinear consequences of exceeding beta limits in NSTX for $q_0 > 1$. Mechanism for soft beta limit identified.
- Sheared rotation is stabilizing
- More violent behavior expected as $q_0 \rightarrow 1$
- Both sawtoothing and m=1 stationary states can occur in resistive MHD depending on transport parameters
- Resistive wall capability available soon
- Convergence studies underway